Ocean Engineering 288 (2023) 116038

Contents lists available at ScienceDirect

Ocean Engineering

journal homepage: www.elsevier.com/locate/oceaneng

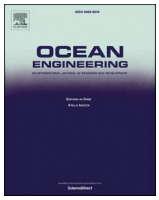

A conflict cluster-based method for collision avoidance decision-making in multi-ship encounter situations

Kezhong Liu [a,b,c], Xiaolie Wu [a,b], Yang Zhou [a,d,*], Zhitao Yuan [a,b], Xing Yang [a,b], Xuri Xin [a,b], Sujie Zhuang [a]

[a] School of Navigation, Wuhan University of Technology, Wuhan, 430063, China
[b] Hubei Key Laboratory of Inland Shipping Technology, Wuhan, 430063, China
[c] National Engineering Research Center for Water Transport Safety, Wuhan University of Technology, Wuhan, 430070, China
[d] Faculty of Civil Engineering and Geosciences, Delft University of Technology, Delft, 2628CN, the Netherlands

ARTICLE INFO

Handling Editor: Prof. A.I. Incecik

Keywords:
Conflict cluster detection
Collision avoidance
Decision-making
Multi-ship encounter

ABSTRACT

During the process of collision avoidance, especially in a multi-ship encounter situation, the dynamic interactions among individual ships impose a significant impact on collision avoidance decision-making. It is imperative, therefore, that collision avoidance decisions are formulated with a comprehensive consideration of not only the current direct collision conflict but also the potential conflicts due to planned collision avoidance actions. To address this requirement, this paper proposes a dynamic conflict cluster detection method for collision avoidance decision-making in multi-ship encounters. The involved ships are clustered into stable temporal-dependent ship conflict groups taking into account both conflict connectivity and the potential spatiotemporal interactions originating from planned collision avoidance actions. The conflict cluster detection model is implemented within a framework to achieve hierarchical coordinated collision avoidance decision-making. By a simulation experiment of an 11-ship encounter, the proposed method successfully discerns the ships with conflicts and provides feasible collision avoidance decisions. Compared to the non-cluster collision avoidance methods, the proposed method generates the results with acceptable deviating distance and number of collision avoidance actions at minimum computation load. It has been demonstrated that the proposed method is both effective and efficient for officers on board and operators at Vessel Traffic Services centers in real-life navigation.

1. Introduction

As one of the major threats to maritime navigation safety, ship collisions may cause severe casualties, economic losses, environmental pollution, etc. Especially in complex waters with heavy traffic flow and intricate ship routes, the occurrence of multi-ship encounters is frequent. Under such circumstances, the probability of ship collisions is anticipated to escalate. For example, in one of the hub ports in China, the Port of Ningbo-Zhoushan, the inbound and outbound ship routes are crossed with a high density of ships, as shown in Fig. 1. Given the distinctive characteristics of ship traffic in such waters, as mentioned above, the issue of collision avoidance during multi-ship encounters has drawn much attention in the research field to enhance navigation safety (Goerlandt et al., 2012; Kulkarni et al., 2020; Yu et al., 2022; Zhang et al., 2016). The objectives primarily encompass two aspects: firstly, to scrutinize potential risks within the region by drawing on historical accidents, thereby providing comprehensive navigational insights; and secondly, to assess real-time local collision risks among ships, enabling collision avoidance decisions to avoid accidents. In pursuit of the latter objective, ships must consider all potential collision candidates, especially in multi-ship encounters.

As revealed by Huang et al. (2020) and Bakdi et al. (2021), the ship collision avoidance techniques can be divided into two stages, *collision risk assessment* and *collision conflict resolution* during encounter process. *The collision risk assessment* aims to identify potential collision candidates and their corresponding collision risks, which is accomplished through three main research approaches: the ship domain-based approach, risk index-based approach, and local risk assessment method. (1) A ship domain refers to an allocated and protected area around a ship where other ships or obstacles are not permitted to intrude or violate. The assessment of collision risk is based on the overlap or violation of ship domains (Rawson and Brito, 2021). The ship domain has been

* Corresponding author. School of Navigation, Wuhan University of Technology, Wuhan, 430063, China.
E-mail address: y.zhou-5@tudelft.nl (Y. Zhou).

https://doi.org/10.1016/j.oceaneng.2023.116038
Received 20 April 2023; Received in revised form 18 September 2023; Accepted 9 October 2023
Available online 19 October 2023

developed in a variety of shapes, such as circular (Fujii and Tanaka, 1971), elliptical (Szlapczynski and Szlapczynska, 2016), fuzzy (Qu et al., 2011; Wang, 2010), or quaternion (Wang, 2013), accounting for various influencing factors. These factors include environmental conditions (Liu et al., 2016), ship maneuverability (Gil et al., 2020; He et al., 2017; Li et al., 2021), knowledge of navigators (Dinh and Im, 2016), traffic situations (Wang and Chin, 2016), etc. The abundant Automatic identification System (AIS) data of ship's dynamic information has significantly enhanced the development of ship domain models and quantitative risk assessment (Kundakçı et al., 2023; R. W. Liu et al., 2022; Rong et al., 2022). However, when a ship uses the ship domain as collision criterion, a collision may be unavoidable due to ship maneuverability (Du et al., 2021; He et al., 2017), making it difficult to be directly applied to collision risk assessment. To solve this problem, ship motion prediction techniques are incorporated, such as linear or nonlinear changes (Chen et al., 2018, 2020) and probability (Li et al., 2022; Park and Kim, 2016; Xin et al., 2021). (2) The index-based method establishes mathematical or black-box models to indicate spatial-temporal proximity of surrounding ships. A collision candidate is identified when the corresponding threshold value of such an index is reached. Among the indices, Distance at the Closest Point of Approach (DCPA) and Time to the Closest Point of Approach (TCPA) are classic ones based on geometrical relationships. Meanwhile, Degree of Domain Violation (DDV), Time to Domain Violation (TDV) (Szlapczynski and Szlapczynska, 2016), as well as Bow Crossing Range (BCR) and Time to Bow Crossing Range (BCT) (Gil et al., 2022), further incorporate ship domain and relative bearing into their calculations. The index-based approaches describe current relative movements among ships, but can hardly be integrated with dynamic ship motions, such as the upcoming collision avoidance actions. (3) The clustering approaches have recently been adopted for local collision risk assessment in multi-ship encounters (Shi et al., 2022; Vu and Jeong, 2021; Zhang et al., 2019; Zhen et al., 2017, 2022a, 2022b). Through this method, ships are clustered with their collision candidates to present local risks. However, the existing clustering approaches are mainly based on traffic density and distance, with only a few studies considering dynamic ship motions and conflict connectivity (Xin et al., 2022, 2023). In high-density waters with crossing ship routes, substantial collision avoidance actions as required by the International Regulations for Preventing Collisions at Sea (COLREGs) may increase collision risk with other ships.

The research on *collision conflict resolution* can be divided into individual ship decision-making and multi-ship coordinated decision-making based on the number of participating entities. Individual-ship collision avoidance research focuses on several aspects, including decision-making optimization (Hu et al., 2020; Johansen et al., 2016; Wang et al., 2020; Zhang et al., 2023), conflict resolution (Cho et al., 2020; Li et al., 2020) and collision-free path planning (Mou et al., 2021; Lyu and Yin, 2019; Tam and Bucknall, 2013; Park et al., 2019). The employed algorithms encompass diverse approaches, such as geometric-based approaches (Chen et al., 2019; Huang et al., 2019; J. Liu et al., 2022; Lyu and Yin, 2019; Perera et al., 2011; Wang et al., 2017), optimization-based approaches (Hu et al., 2019; Kang et al., 2018; Lazarowska, 2015; Liu et al., 2017; Szlapczynski, 2011; Tsou, 2016), reinforcement learning approaches (Shen et al., 2019; Woo and Kim, 2020; Zhao and Roh, 2019), etc. In multi-ship encounters, the relative movement between ships probably keeps changing due to the actions taken by any involved ships, which affects the decision-making and may lead to incorrect decisions. With the advancement of communication technologies, ship-to-ship route exchange through Very High Frequency radio and other advanced communication systems has been thoroughly investigated and is on the verge of implementation (Akdağ et al., 2022). Hence, based on exchanging collision avoidance information among ships, coordination decision-making methods have been developed for multiple ships to achieve the efficiency and consistency. These coordination methods include distributed coordination strategy (Li et al., 2019), distributed multi-ship anti-collision decision system (Zhang et al., 2015), distributed search method (Kim et al., 2014, 2017), and cooperative path planning algorithm (Tam and Bucknall, 2013).

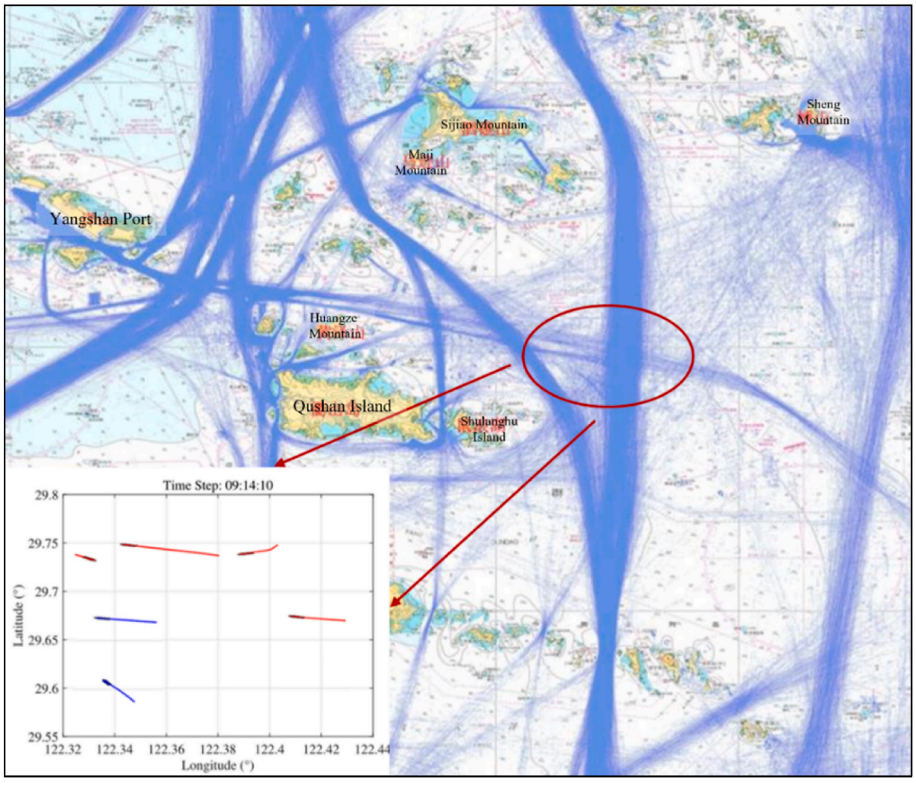

Fig. 1. The ship traffic on 15 August 2022 in the Port of Ningbo-Zhoushan, China.. (The zoom-in window presents a multi-ship encounter in the area with crossing ship routes.)

However, as the number of involved ships increases in multi-ship encounters, achieving coordination for all involved ships can be challenging due to the technical issue of high computation loads and the practical reason of probable insufficient communication in real-life navigation (Cho et al., 2020; Kim et al., 2014).

To address the aforementioned limitations of existing research on collision avoidance decision-making in high-density waters with complex ship routes, especially for multi-ship encounters, this paper proposes *a dynamic conflict cluster detection method*. Such a conflict cluster collects the ships with significant interactions for the current collision avoidance decision-making. Specifically, the main contributions of this paper are triple: (1) The proposed cluster detection method identifies ship clusters by considering both the immediate direct conflicts and the upcoming potential conflict arising from collision avoidance actions, which is important for both ship officers on board and traffic managers; (2) The conflict cluster detection method is implemented to hierarchically and efficiently achieve coordinated collision avoidance decision-making in multi-ship encounter situations; (3) Compared to the non-cluster collision avoidance methods, the proposed method demonstrates a favorable balance between safety, economy, and computation load, thereby aligning with practical application needs.

The remainder of this paper is organized as follows. Section 2 introduces the relevant definitions of this research and the underlying assumptions, followed by a detailed explanation of the proposed methodology in Section 3. The setup of the simulation experiments and the discussions on the results are presented in Section 4. Finally, Section 5 concludes the paper and directs possible future research.

2. Definitions and assumptions

As previously stated, this paper aims to detect the clusters of ships with conflicts in multi-ship encounters situations from all surrounding ships in complex and busy sailing environments. The purpose of detection is to identify both the current direct conflicts and the upcoming potential conflicts due to the expected Collision Avoidance (CA) actions. To be specific, a *direct conflict* refers to the situation where one ship (*Ship i*) will shortly violate the domain of another ship (*Ship j*) if both ships maintain their current speed and course, while a *potential CA conflict* refers to the situation where the *CA path* planned by either ship with a direct conflict (*Ship i* or *Ship j*) will violate the domain of a third ship (*Ship k*), as shown in Fig. 2.

To illustrate the detection result, a *conflict cluster* refers to a collection of ships with significant interaction for the current CA decision-making, including the ships with a direct conflict and/or a potential CA conflict. An example of the conflict clusters is presented in Fig. 3. The ships with direct conflicts are marked in red and linked by solid red lines, while the ships with potential CA conflicts are in yellow and linked by dashed black lines. To be more specific, *Ship* S_7 will be involved in collision risks due to the CA actions of *Ship* S_3, and *Ship* S_8 will be affected by the CA actions of *Ship* S_1 and *Ship* S_9. Besides, since *Ship* S_1 will encounter *Ship* S_8 after she completes her current CA action, for the current time being, there exists no significant CA interaction between *Ship* S_1 and *Ship* S_8, as they belong to different clusters. Thus, the situation concerning ten ships is divided into three conflict clusters, each encircled by red circles to assist their CA decision-making.

During the conflict cluster detection process, several assumptions have been posited in this research:

(1) The shape of the ship domain is simplified as a circle with a radius of six times the ship length;
(2) The CA action refers to course alteration only;
(3) The ships are assumed to exchange information about their CA actions.

The design of circular ship domain is intended to guarantee a basic safety distance from other ships, which has been widely adopted in the field of collision avoidance research (Cho et al., 2020; Johansen et al., 2016; J. Liu et al., 2022; Lyu and Yin, 2019). In the future, the shapes considering more influencing factors, such as ship type and size, can be incorporated into the proposed methodology.

As suggested by COLREGs and observed in practical navigation, if the collision risk can be judged at an early stage, course alteration will be the preferred option for CA actions (Gil et al., 2020; Li et al., 2019; J. Liu et al., 2022; Lyu and Yin, 2019). Furthermore, owing to large inertia, the impact of deceleration requires a long stopping distance (He et al., 2017). In the case of an emergency to avoid the immediate danger of collision, it is necessary for ships to change both course and speed as CA actions. However, this paper specifically focuses on the study of course alteration at early stages, in accordance with the suggestions of COLREGs.

Lastly, the International Maritime Organization has implemented the e-navigation projects, which aim to develop innovative communication technologies. As a prerequisite, the exchange CA actions between all vessels is assumed. The information, including ship position, speed, course, and planned paths of all involved ships, is exchanged through communications.

3. Research methodology

In this section, the overall framework for CA decision-making is elaborated in detail, as illustrated in Fig. 4. Firstly, the conflict clusters

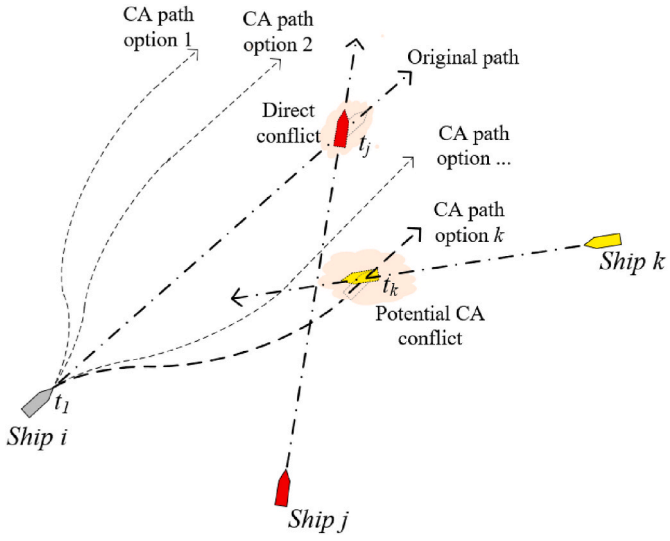

Fig. 2. Illustration of a potential CA conflict.. (A *direct conflict* exists between *Ship i* and *Ship j*. Due to the CA path option *k* by *Ship i*, a *potential CA conflict* is formed between *Ship i* and *Ship k*.)

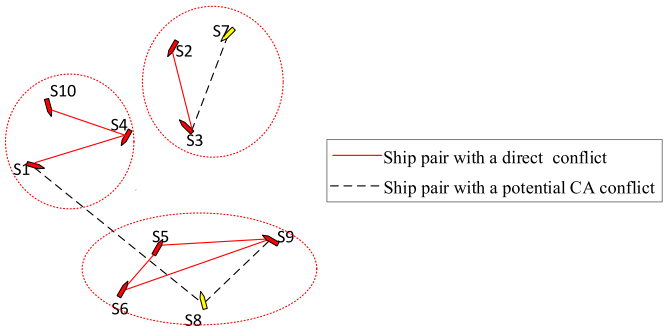

Fig. 3. Illustration of the definitions of conflict clusters: [S_2, S_3, S_7], [S_{10}, S_4, S_1], [S_6, S_5, S_9, S_8]. (The ships with direct conflicts are marked in red, while the ones with potential CA conflicts are in yellow).

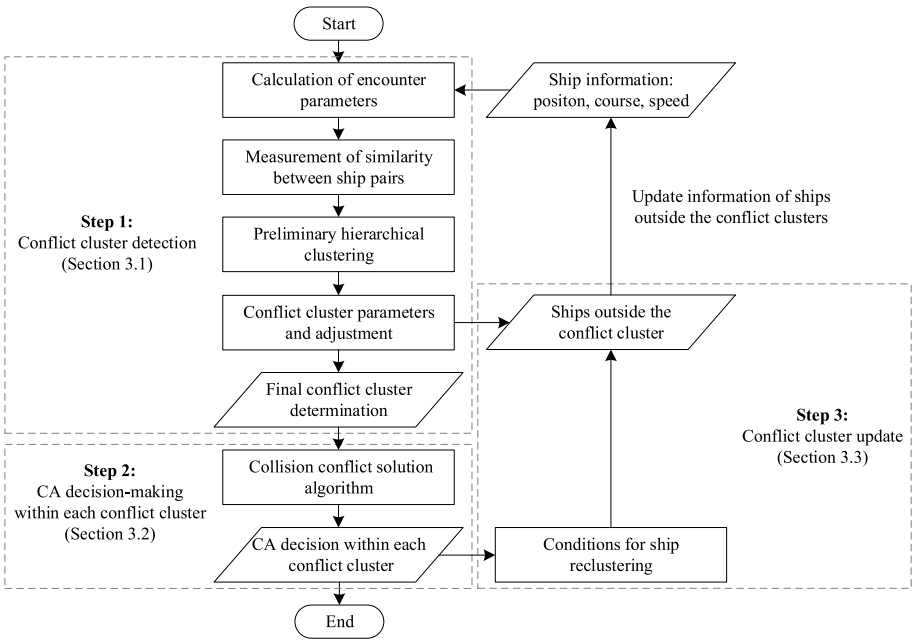

Fig. 4. Overview of the proposed approach.

are preliminarily detected according to the similarity measurement between ship pairs. This measurement depends on the calculated parameters describing the encounter situation in Step 1. The coordinated CA decision is then formulated within each conflict cluster as explained in Step 2. Step 3 introduces the conditions to update the conflict clusters and the dynamic movement information of all ships, including those both within and outside the clusters.

3.1. Conflict cluster detection

In this subsection, the process of conflict cluster detection is introduced, containing the calculation of encounter parameters in Section 3.1.1, the measurement of similarity between ship pairs in Section 3.1.2, the preliminary identification of conflict clusters by hierarchical clustering in Section 3.1.3 and the final determination by conflict cluster parameters in Section 3.1.4.

3.1.1. Calculation of encounter parameters

According to the definitions of direct conflict and potential CA conflict in Section 2, the parameters used to characterize an encounter vary depending on the type of detected collision conflict. The parameters are introduced as follows, respectively.

3.1.1.1. Parameters for encounters with a direct conflict. In maritime domain, DCPA and TCPA are two common indices used to delineate the collision risk between ships during an encounter from a spatial-temporal perspective. However, given that TCPA pertains to the time to the closest point of approach, it occurs after the instance of domain invasion by either ship. According to Szlapczynski and Szlapczynska (2016), two indices are introduced to describe the relationship based on domain violation are introduced, being DDV and TDV. DDV describes the violation degree of the own ship's domain by the target ship using a scale factor approach $f_{\min}$, to calculate the scale of domain invasion when the target ship crosses the boundary of the own ship's domain. As defined, the value of DDV is determined by $\max(1 - f_{\min}, 0)$. From a temporal viewpoint, TDV signifies the remaining time for the target ship to enter the domain of the own ship, assuming both ships maintain their course and speed. As mentioned in Section 2, the shape of ship domain in this research is assumed to be a circle with a radius of R_d.

To provide a more stringent explanation, as shown in Fig. 5, the

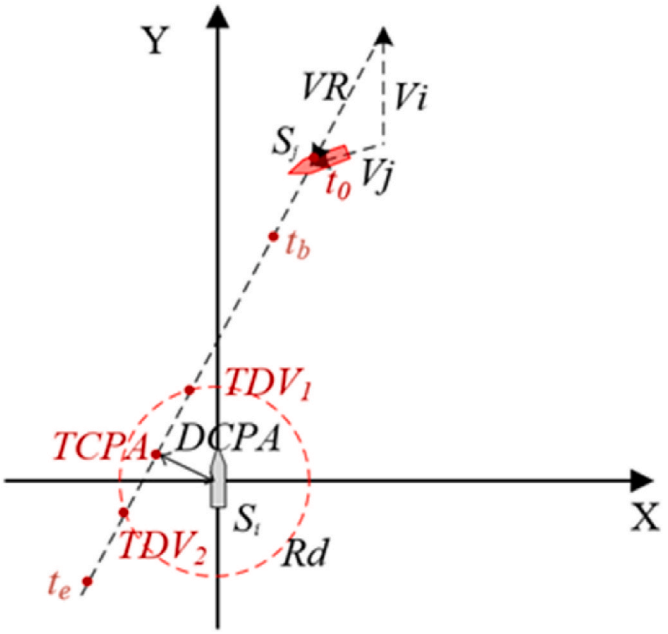

Fig. 5. Illustration of parameters to describe the encounter with a conflict. (t_0, t_b, TDV_1, TDV_2, and t_e represent different time steps during the encounter process, while *TCPA* indicates the time to the closest point of approach.)

definitions are illustrated further. If both ships in the pair $pair(S_i, S_j)$ maintain their course and speed as they are at the initial time t_0, *Ship* S_j will violate the domain of *Ship* S_i at the time TDV_1 and leave at the time TDV_2. To contextualize the temporal aspect of ships' interaction, the Time Window of Conflict (TWC) is introduced, which refers to the period $[t_b, t_e]$. During this defined timeframe, a conflict is determined according to *DDV*, TDV_1, and TDV_2.

The relevant parameters are calculated as follows,

$$DDV = 1 - \frac{DCPA}{R_d} \tag{1}$$

$$TDV_1 = \begin{cases} TCPA - \dfrac{\sqrt{R_d{}^2 - DCPA^2}}{VR}, DDV \geq 0 \\ TCPA - \dfrac{\sqrt{DCPA^2 - R_d{}^2}}{VR}, DDV < 0 \end{cases} \quad (2)$$

$$TDV_2 = \begin{cases} TCPA + \dfrac{\sqrt{R_d{}^2 - DCPA^2}}{VR}, DDV \geq 0 \\ TCPA + \dfrac{\sqrt{DCPA^2 - R_d{}^2}}{VR}, DDV < 0 \end{cases} \quad (3)$$

where VR is the relative speed of *Ship* S_j to *Ship* S_i; R_d is the radius of circular domain; $DCPA$ and $TCPA$ can be calculated according to the position and speed of both ships.

Based on the calculation results, if two criteria (1) $DDV > 0$ and (2) $TDV_2 > 0$ are both met, a *direct conflict* is identified between the ship pair $pair(S_i,S_j)$. If either criterion is not satisfied, it is deemed as no direct conflict exists between the pair.

As regulated in *Rule 16* (*Action by Give-way Vessel*) of COLREGs, the give-way ship shall, as far as possible, take early and substantial action to keep well clear. Therefore, once a *direct conflict* is identified ($DDV > 0$ and $TDV_2 > 0$), the time period of ship interaction TWC for the ship pair $pair(S_i, S_j)$ is defined as

$$TWC_{ij} = [t_b, t_e] \quad (4)$$

where $t_b \in [0, TDV_1 - \tau_1]$ refers to the beginning of the influence by *Ship* S_j, and $t_e = TDV_2 + \tau_2$ refers to the end of the interaction, in which τ_1 and τ_2 are constant. The value of t_b will be explained in Section 3.1.4.

3.1.1.2. Parameters for encounters with a potential CA conflict. To describe the encounter with a *potential CA conflict*, an example is illustrated in Fig. 6. The CA path set {*CA path* 1, *CA path* 2, …, *CA path option n*} of *Ship* S_i includes a series of planned CA paths constrained in the confined space, in which *CA path 2* may violate the domain of *Ship* S_k at the Possible Point of Collision (PPC_2). The point Pr_2 refers to the point when *Ship* S_i returns to her initial course. This point can be deemed as equivalent to sailing from the position of the virtual ship S_{i_2} with the original course. As shown in Fig. 6, the following can be proved:

$$\begin{cases} \widehat{S_iPr_2} = \overline{S_{i\_2}D_2} + \overline{D_2Pr_2} \xrightarrow{yields} \overline{D_{CA}} > \overline{S_iD_2} > \overline{S_{i\_2}D_2} \\ \overline{S_iD_2} + \overline{D_2Pr_2} > \widehat{S_iPr_2} \end{cases} \quad (5)$$

where $\widehat{S_iPr_2}$ means curve distance of the CA path from the point S_i to the point Pr_2 by *Ship* S_i; the point D_2 marks the intersection of the starboard abeam of *Ship* S_i and the path by virtual *Ship* S_{i_2}; $\overline{S_iD_2}$ refers to the linear distance between the point S_i and D_2; $\overline{S_{i\_2}D_2}$ refers to the linear distance between S_{i_2} and D_2; $\overline{D_2Pr_2}$ refers to the linear distance between D_2 and Pr_2; and $\overline{D_{CA}}$ indicates the CA space constraint.

Since the position of the virtual *Ship* S_{i_2} is within the range of D_{CA} astern and on both sides of the real *Ship* S_i, the length of $\overline{S_{i\_2}D_2}$ is smaller than $\overline{D_{CA}}$. The same goes for other CA path options. As a result, the CA space for the equivalent virtual ships is presented as the yellow rectangular area around the real *Ship* S_i in Fig. 6.

As shown in Fig. 7, TC_i indicates the true course of *Ship* S_i, while *Ship* S_k approaches *Ship* S_i along the direction of relative velocity VR. Although the domain of *Ship* S_k will not be invaded by *Ship* S_i, the domain still overlaps with the CA space for equivalent virtual ships of *Ship* S_i in the dashed yellow rectangular. It means the CA actions by *Ship* S_i may interfere with *Ship* S_k, which forms a *potential CA conflict*. During this type of encounter, the period with interaction influence is defined as $TWC_{ij} = [t_b', t_e']$.

In XOY system, the coordinates of $P(X, Y)$ and the position of *Ship* S_k fulfill the relationship:

$$\begin{cases} (X - px_k(t))^2 + (Y - py_k(t))^2 = R_d{}^2 \\ py_k(t) - py_k(t_0) = \dfrac{VR_x}{VR_y}(px_k(t) - px_k(t_0)) \\ px_k(t) = px_k(t_0) + VR_x \cdot t \end{cases} \quad (6)$$

where $(px_k(t_0), py_k(t_0))$ and $(px_k(t), py_k(t))$ refer to the position of *Ship* S_k at the current time t_0 and time step t; VR_x and VR_y are the projected components of VR; R_d is the domain radius of *Ship* S_k.

In the attached coordinate system *xoy*, the intersection point $P(x,y)$ follows the basic conditions:

$$-D_{CA} < x < D_{CA} \text{ and } -D_{CA} < y < 0 \quad (7)$$

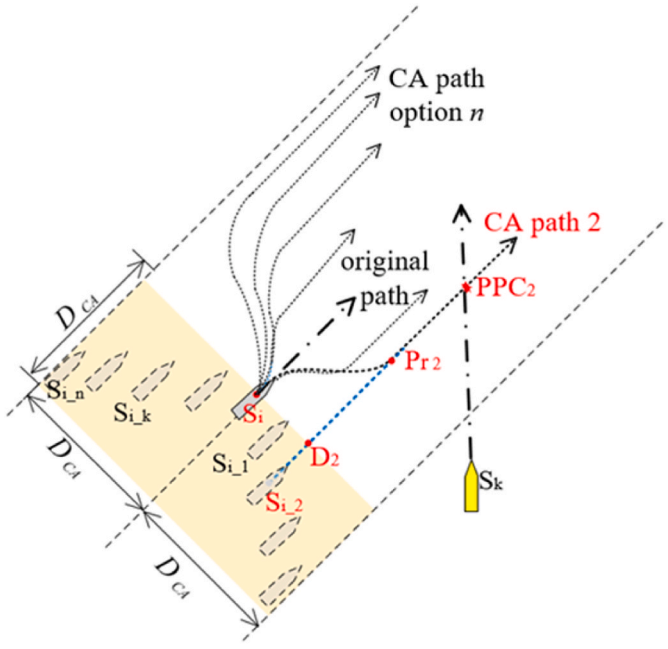

Fig. 6. Equivalent virtual ship position for a potential CA conflict from the perspective of a true movement of *Ship* S_i and *Ship* S_k. (S_i and S_k represent real ships; $S_{i\_1}, \ldots, S_{i\_n}$ are virtual ships of S_i for CA path options.) (A potential CA conflict exists between *Ship* S_i and *Ship* S_k due to the domain invasion of CA path 2 by *Ship* S_i with *Ship* S_k at the point PPC_2.).

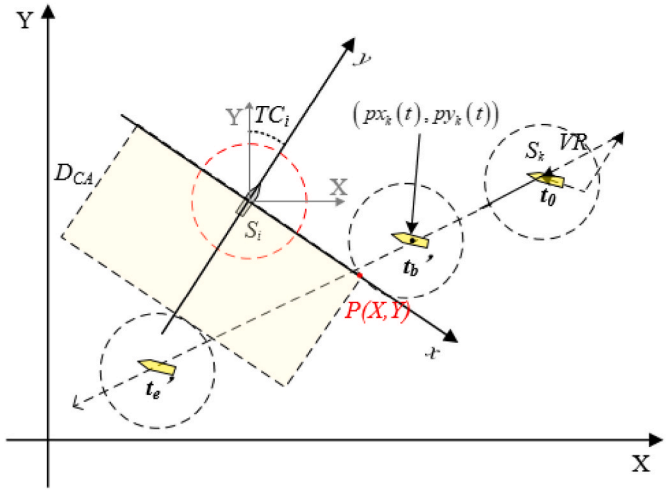

Fig. 7. Illustration of parameters to describe the encounter with a *potential CA conflict* between *Ship* S_k and *Ship* S_i. (The coordinate system XOY is fixed to the earth, while the system *xoy* is attached to *Ship* S_i. The point $P(X, Y)$ represents the intersection between the CA space of *Ship* S_i and the domain of *Ship* S_k.)

Therefore, the position of the virtual *Ship* S_i in XOY system can be converted to *xoy* system by:

$$[X, Y] = [x, y] \cdot A + [px_i(t_0), py_i(t_0)] \tag{8}$$

where the transformation matrix refers to $A = \begin{bmatrix} \cos(TC_i) & -\sin(TC_i) \\ \sin(TC_i) & \cos(TC_i) \end{bmatrix}$, $[px_i(t_0), py_i(t_0)]$ is the position of *Ship* S_i at the current time t_0 in *xoy* system, while D_{CA} represents the spatial boundary of CA space.

The geometrical relationship between the CA space of *Ship* S_i and the domain of *Ship* S_k can be indicated by the solution of $[X, Y]$ through Eqs. (6)–(8). If no solution of $[X, Y]$ can be achieved, it indicates that the absence of an intersection point, as depicted in Fig. 8 (a), implies no plausible potential CA conflict between *Ship* S_i and S_k. If only one solution of $[X, Y]$ is present, as depicted in Fig. 8 (b) and (c) (only one intersection point $P(X, Y)$), a potential CA conflict exists. By Eq. (6), the threshold value of TWC_{ik} can be obtained. In cases where there is more than one solution of $[X, Y]$, as shown in Fig. 8 (d) (more than one intersection point), it signifies the presence of a potential CA conflict, with *Ship* S_i being interfered by *Ship* S_k.

In multi-ship encounter situations where there exist both direct conflicts and potential CA conflicts, the ending time of *TWC* can be calculated by the time when the give-way ship is past and clear, i.e., $t_e^{'} = t_e$.

3.1.2. Measurement of similarity between ship pairs

To measure the similarity between ship pairs, the distance between *TWC* of ships in different situations is defined as follows.

(1) If there is a common ship S_i between two pairs with different types of conflict, given $pair(S_i, S_j)$ with a direct conflict and $pair(S_i, S_k)$ with a potential CA conflict, the time windows *TWC* for two pairs are $TWC_{ij} = [t_b, t_e]$, $TWC_{ik} = [t_b^{'}, t_e^{'}]$, respectively. The distance between the ship pairs can be calculated:

$$dis\big(pair(S_i, S_j), pair(S_i, S_k)\big) = \begin{cases} 0, t_b < t_e^{'} \text{ and } t_e < t_b^{'} \\ \min(|t_b^{'} - t_e|, |t_e^{'} - t_b|), \text{others} \end{cases} \tag{9}$$

(2) If there is no common ship between two ship pairs, given $pair(S_i, S_j)$ with a direct conflict and $pair(S_m, S_n)$ with a potential CA conflict, the distance of two ship pairs is defined as positive infinity.

Taking *Ship* S_0 as the own ship in Fig. 9, the conflicts in multi-ship encounter situations can be analyzed as follows: a direct conflict exists between the ship pair (S_0, S_3) shown in red, while potential CA conflicts exist among the pairs (S_0, S_1), (S_0, S_2), and (S_0, S_4) presented in blue. Fig. 9 also shows the temporal sequences of the interactions between the ships from the current time t_0 to the estimated ending time t_{end}. During the process, the point TDV_1 indicates the time of domain violation by *Ship* S_3 due to the direct conflict; while t_b refers to the start time of interaction by *Ship* S_3 and t_3 refers to the ending time of the interaction. Similarly, the time window *TWC* of the ship pairs (S_0, S_1), (S_0, S_2), and (S_0, S_4) can be represented as $[t_0, t_1]$, $[t_2, t_4]$, and $[t_5, t_{end}]$, respectively. According to the definition of distance between the pair with a direct conflict and each pair with a potential CA conflict, distances between the pairs can be determined as follows:

$$dis(pair(S_0, S_3), pair(S_0, S_1)) = 0 \tag{10}$$

$$dis(pair(S_0, S_3), pair(S_0, S_2)) = 0 \tag{11}$$

$$dis(pair(S_0, S_3), pair(S_0, S_4)) = t_5 - t_3 \tag{12}$$

3.1.3. Preliminary hierarchical clustering

Based on the similarity measurement between ship pairs in Section 3.1.2, a preliminary result of ship clustering can be obtained by the hierarchical clustering process, which is presented in **Algorithm 1**.

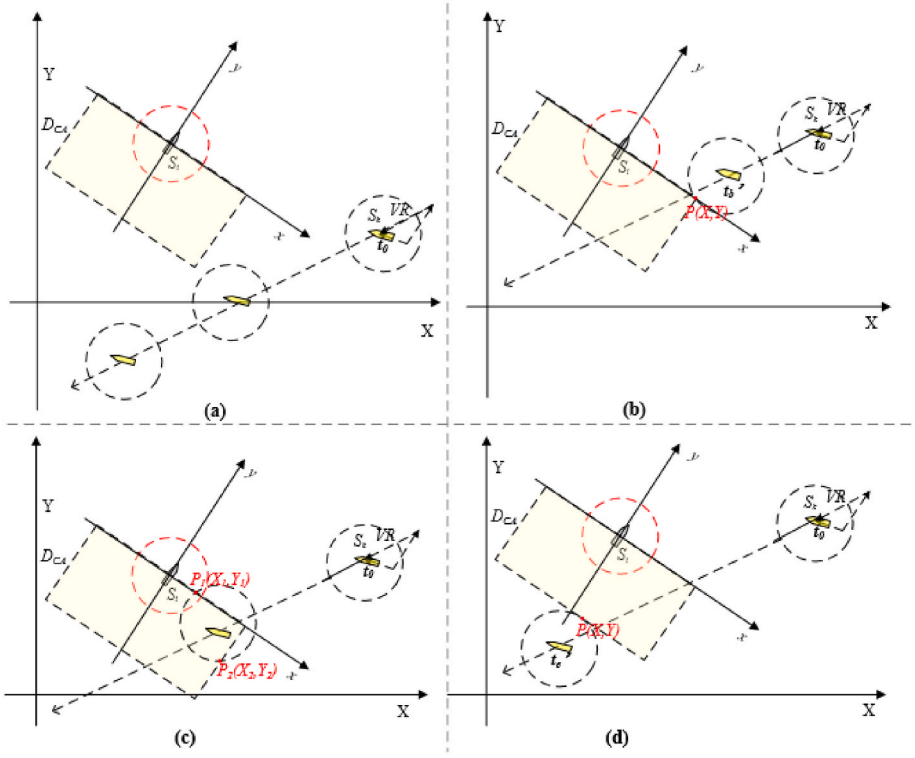

Fig. 8. Illustration of encounters when judging a potential CA conflict. (a. no potential CA conflict with no intersection point; b. the starting time of the potential CA conflict indicated by only one intersection point $P(X, Y)$; c. the ongoing process of the potential CA conflict indicated by more than one intersection point; d. the ending time of the potential CA conflict indicated by only one intersection point $P(X, Y)$.)

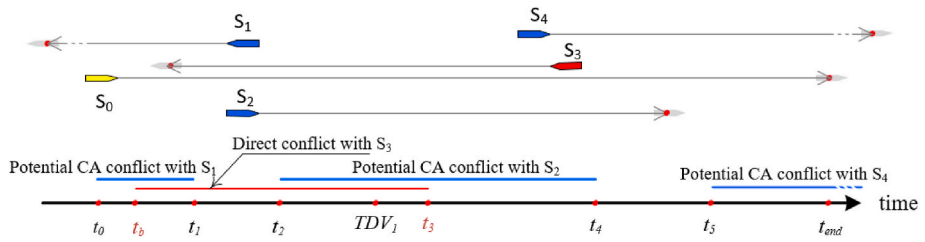

Fig. 9. Illustration of the interactions in a multi-ship encounter taking *Ship* S_0 as the own ship (The ships and lines in red represent the ships with a direct conflict with *Ship* S_0, while the ones in blue for the ships with a potential CA conflict with *Ship* S_0).

Algorithm 1. Algorithm of the preliminary hierarchical ship clustering.

By calculating the similarity matrix and simplifying it to a binary-tree-like hierarchical index matrix, the encountered ships are preliminarily clustered into several clusters including all ships with either type of conflict.

3.1.4. Final cluster determination

Following an examination of the preliminary clustering result, it is necessary to conduct a thorough investigation into the parameters used to describe the state of clusters as well as the constraints guiding CA decision-making among clusters. This investigation is crucial in order to determine the final conflict clusters accurately. The purpose of conflict cluster detection is to facilitate the coordinated CA decisions of ships in multi-ship encounters. The computation load is expected to be higher when more ships are clustered in one group. In this research, the parameters include the deviating distance D_{CA}, the beginning time of interference between the ships t_b, and the time for the ships to be past and clear t_c.

(1) Deviating distance D_{CA}.

The deviating distance describes the CA space of a ship as shown in Fig. 6, which is used to judge whether there exists a potential CA conflict and calculate *TWC* for each ship pair with conflicts. A larger value of D_{CA} for the own ship will result in more ships getting involved in potential CA conflicts with the ship. In other words, a positive relationship exists between the deviating distance D_{CA} and the number of ships in the cluster n_{in}^k.

When ships are preliminarily clustered, the maximum deviation of CA path options by the own ship must be smaller than D_{CA}. It means all ships with potential CA conflicts due to any CA options are included in the cluster. Thus, the deviating distance D_{CA} is adopted to assess the preliminary clustering result.

(2) Beginning time of interference t_b.

When there exists a direct conflict between the ships $pair(S_i, S_j)$, the beginning time of interference between the ships $t_b \in [0, TDV_1(S_i, S_j) - \tau_1]$, is stated in Section 3.1.1. In a ship cluster, an earlier beginning time of interference t_b means a longer time window of conflict between the pair TWC_{ij}. Under such circumstances, the probability of conflict interference with other ship pairs is also larger, which also leads to more ships getting involved in the cluster. Consequently, a negative relationship exists between the value of the beginning time t_b and the number of ships in the cluster n_{in}^k.

Considering the requirement of taking early CA actions in COLREGs, the earliest interference t_b starts from the current time t_0, which is the second constraint to determine the ships in clusters.

(3) **Time of being past and clear** t_c.

The process of an encounter with CA actions finishes when two ships get past and clear, as required by *Rule 8* in COLREGs. Therefore, an additional parameter needs to be defined to determine the moment, which is the time for both ships being past and clear t_c in this research. If the time being is earlier than this moment, it implies that the own ship remains entangled in conflicts with certain ships within the cluster. This parameter represents the threshold in the hierarchical clustering tree. Thus, the relationship between the time being past and clear t_c and the number of ships in the cluster n_{in}^k is positive.

Considering the requirement by COLREGs, the value t_c is defined as a gradual decrease from 10 min by default. This is also the last constraint to determining the ships in clusters.

3.2. CA decision-making within conflict clusters

The purpose of conflict cluster detection is to make coordinated CA decisions within the clusters in multi-ship encounters. The process is

1: Initial state

2: $\mathcal{S} \leftarrow \{s_1, s_2, \cdots, s_n\}$ \\ $\mathcal{S}$ refers to the ships with a direct conflict and/or a potential CA conflict.

3: $c_m \leftarrow TWC_{ij}$ \\ TWC_{ij} refers to the time window of conflict for $pair(s_i, s_j)$, which is sorted and marked as c_m.

4: $\mathcal{C} \leftarrow \{c_1, c_2, \cdots, c_m\}$, \\ $\mathcal{C} = (c_i)_{2\times m}$ describes the ship pairs with either type of conflict.

5: $E \leftarrow \{e_{11}, e_{12}, \cdots, e_{mm}\}$ \\ E= $(e_{gh})_{m\times m}$ indicates the conflict edges, where e_{gh} refers to the similarity between ship pairs with conflicts c_g and c_h.

6: $G = (C, E)$ \\ Ship pairs with conflicts C form a network G with conflict edges E.

7: $E\_bt = (e\_bt_{ij})_{(m-1)\times 3}$ \\ returning a binary-tree-like hierarchical index matrix E_bt from G.

8: $E^k = \{c_1, c_2, \cdots, c_m\} \leftarrow$ FIND all ship pairs c_i *if* $E\_bt(:,3) < t_c$ and save the results in E^k. \\$t_c$ refers to the time threshold.

9: $\mathcal{S}_{in}^k = \{s_1, s_2, \cdots, s_n\} \leftarrow$ FIND all ships s_i in E^k\\ $\mathcal{S}_{in}^k$ collects the ships within the conflict clusters k.

10: Output $\mathcal{S}_{in} \leftarrow \{\mathcal{S}_{in}^1, \mathcal{S}_{in}^2, \cdots, \mathcal{S}_{in}^k\}$, $\mathcal{S}_{out} \leftarrow \mathcal{S} \backslash \mathcal{S}_{in}$ \\$\mathcal{S}_{in}$ collects all ships within any conflict cluster and $\mathcal{S}_{out}$ include the ships out of all conflict clusters.

explained in detail as follows. Section 3.2.1 introduces the overall framework of decision-making based on the detected conflict clusters. The processes to make optimal CA decisions for individual ships in each cluster and to make coordinated CA decisions are explained in Section 3.2.2 and Section 3.2.3, respectively.

3.2.1. Overall framework

The coordinated CA decisions are achieved and updated based on the results of conflict cluster detection, which can be presented in two steps:

(1) Update the state of cluster detection for all ships, including the ships outside all clusters $\mathscr{S}_{out}$ and the ships in the corresponding clusters $\mathscr{S}_{in} = \{\mathscr{S}_{in}^1, \mathscr{S}_{in}^2, \cdots, \mathscr{S}_{in}^k\}$, where $\mathscr{S}_{in}^l$ represents all ships in cluster l;
(2) Update the CA decisions for ships in each cluster by distributed coordination strategy.

At the beginning of a multi-ship encounter, all involved ships can be deemed as outside any cluster, which is $\mathscr{S}_{out}$. Applying the steps for cluster determination in Section 3.1, the ships are divided into conflict clusters $\mathscr{S}_{in}$. Within each cluster $\mathscr{S}_{in}^l$, CA decisions are formulated based on Particle Swarm Optimization (PSO) algorithm.

Algorithm 2. The overall framework for CA decisions based on conflict cluster detection.

3.2.2. Optimal CA decision for individual ships

The CA decisions for individual ships within each cluster are achieved by PSO algorithm. To apply the algorithm, variables, constraints, and objective functions for optimization are explained in detail.

3.2.2.1. Variables for CA actions. A CA process assists in ascertaining appropriate action to avoid collisions at a specific time. The alteration of course is widely recognized as an efficacious maneuver for implementing ship collision avoidance techniques. To figure out the CA decisions within each cluster, three action variables $[t_a, \Delta TC, t_r]$ are selected for optimization, as illustrated in Fig. 10. The action time t_a refers to the period from ship's current position P_0 to the point of course alteration P_1; ΔTC is the magnitude of course change, with a positive value

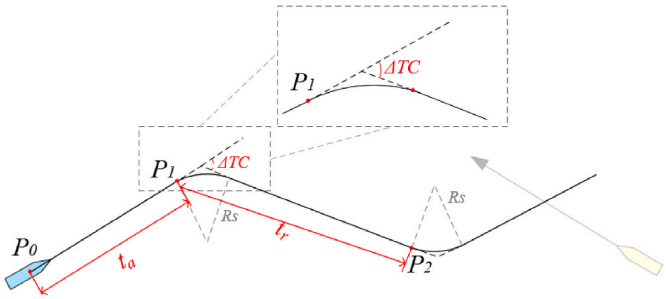

Fig. 10. The illustration of optimization variables for CA decision.

indicating a starboard-side turn, and a negative value indicating a port-side turn; the recovery time t_r means the time period from the position of course alteration P_1 to the point of course recovery P_2; R_s is the simplified ship maneuvering radius, meaning that after an evasive action, the ship cannot immediately reach the new course but gradually achieves it along an arcuate trajectory. For instance, a ship makes a CA decision [5 min, +30°, 15 min] at position P_0 at the time 1200. It means that the ship will initiate a starboard turn of 30° at 1205 at the predicted position P_1. Subsequently, the ship will recover its original course at 1220 at the predicted position P_2.

In this research, *DDV* to a target ship is adopted to estimate the conflict risk. Currently, a majority of risk models for CA decisions assume that other ships shall maintain their speed and course, neglecting the consideration of potential CA paths taken by other ships. Nevertheless, it is not realistic to coordinate decision-making within one cluster. To address this problem, a scheme for the CA path in phases is proposed, as presented in Fig. 11. When one ship has made her own CA decision in the preceding round of coordination, the decision-making of the other ship in the subsequent round needs to take into account the planned decision and action option. As shown in Fig. 11, the CA paths are calculated in five phases, i.e., $\{t_0 \sim t_1, t_1 \sim t_2, t_2 \sim t_3, t_3 \sim t_4, t_4 \sim t_5\}$.

The detailed calculation of the time and position is shown in Table 1, where P_{i_u} and t_u refer to the position of Ship S_i at the uth time; $[t_{ai}, \Delta TC_i, t_{ri}]$ are the variables for CA decision-making considering the dynamic ship information, including steering radius R_{si}, speed v_i , and course TC_i

1: Initial state
2: $\mathcal{S}_{out} \leftarrow$ all involved ships \\ $\mathcal{S}_{out}$ refers to the ships outside all clusters, which are all involved ships at the initial state.
3: $\mathcal{S}_{in} \leftarrow \{\mathcal{S}_{in}^1, \mathcal{S}_{in}^2, \cdots, \mathcal{S}_{in}^k\}$ \\$\mathcal{S}_{in}$ refers to the ships in clusters composed of each group of ships $\mathcal{S}_{in}^l$, which is empty at the initial state.
4: for each t_u \\ at each time step
5: for each $\mathcal{S}_{in}^l$ in $\mathcal{S}_{in}$
6: Run PSO algorithm for $\mathcal{S}_{in}^l$; \\ CA decision-making for individual ships within each cluster for $\mathcal{S}_{in}^l$.
7: if *Ship* S_i in $\mathcal{S}_{in}^l$ triggers the conditions for ship reclustering in Section 3.3
8: then $\mathcal{S}_{out} \leftarrow \mathcal{S}_{out} \cup \{Ship\ S_i\}$, $\mathcal{S}_{in}^l \leftarrow \mathcal{S}_{in}^l \backslash \{Ship\ S_i\}$ \\ add *Ship* S_i into $\mathcal{S}_{out}$ and delete *Ship* S_i from $\mathcal{S}_{in}^l$
9: end if
10: if $\mathcal{S}_{in}^l = \emptyset$ \\ if $\mathcal{S}_{in}^l$ is empty, $\mathcal{S}_{in}^l$ is dissolved
11: then $\mathcal{S}_{in} \leftarrow \mathcal{S}_{in} \backslash \{\mathcal{S}_{in}^l\}$ \\ delete $\mathcal{S}_{in}^l$ from $\mathcal{S}_{in}$
12: end if
13: end for $\mathcal{S}_{in}^l$
14: Run **Algorithm 1** for final cluster determination to obtain $\mathcal{S}_{out}$ \\ conflict cluster detection for all ships in $\mathcal{S}_{out}$
15: $\mathcal{S}_{in} \leftarrow \mathcal{S}_{in} \cup \mathcal{S}_{in}'$, $\mathcal{S}_{out} \leftarrow \mathcal{S}_{out}'$ \\ $\mathcal{S}_{in}'$ and $\mathcal{S}_{out}'$ are the reclustering output of cluster determination
16: end for t_u

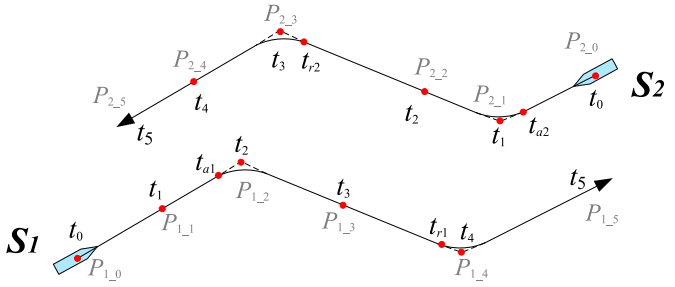

Fig. 11. The scheme of CA paths in phases for a pair of ships. (P_{i_u} refers to the position of Ship S_i at time t_u; t_{ai} and t_{ri} are the action time and recovery time of Ship S_i.)

Table 1
The calculation of time and position for both ships in different CA phases.

Time	Position
$t_1 = t_{a2} + \frac{R_{s2} rad(\Delta TC_2)}{2v_2}$	$P_{1\_1} = P_{1\_0} + (v_1 t_{a2}) \bullet [\sin(TC_1), \cos(TC_1)]$ $P_{2\_1} = P_{2\_0} + [v_2 t_{a2} + R_{s2} \tan(\Delta TC_2/2)] \bullet [\sin(TC_2), \cos(TC_2)]$
$t_2 = t_{a1} + \frac{R_{s1} rad(\Delta TC_1)}{2v_1}$	$P_{1\_2} = P_{1\_0} + (v_1 t_{a1} + R_{s1} \tan(\Delta TC_1/2)) \bullet [\sin(TC_1), \cos(TC_1)]$ $P_{2\_2} = (t_2 - t_1)(P_{2\_3} - P_{2\_1})/(t_3 - t_1)$
$t_3 = t_1 + t_{r2}$	$P_{1\_3} = (t_3 - t_2)(P_{1\_4} - P_{1\_2})/(t_4 - t_2)$ $P_{2\_3} = P_{2\_1} + [v_2 t_{r2} - R_{s2} rad(\Delta TC_2) + 2R_{s2} \tan(\frac{\Delta TC_2}{2})] \bullet [\sin(TC_2 + \Delta TC_2), \cos(TC_2 + \Delta TC_2)]$
$t_4 = t_2 + t_{r1}$	$P_{1\_4} = P_{1\_2} + [v_1 t_{r1} - R_{s1} rad(\Delta TC_1) + 2R_{s1} \tan(\frac{\Delta TC_1}{2})] \bullet [\sin(TC_1 + \Delta TC_1), \cos(TC_1 + \Delta TC_1)]$ $P_{2\_4} = P_{2\_3} + [v_2(t_4 - t_3) - R_{s2} rad(\Delta TC_2)/2 + R_{s2} \tan(\Delta TC_1/2)] \bullet [\sin(TC_2), \cos(TC_2)]$

of *Ship* S_i. The turning maneuver for *Ship* S_i is simplified by geometric calculations. For example, the time t_1 is calculated as $t_1 = t_{a2} + \frac{R_{s2} rad(\Delta TC_2)}{2v_2}$, while the position is $P_{2\_1} = P_{2\_0} + [v_2 t_{a2} + R_{s2} \tan(\Delta TC_2/2)] \bullet [\sin(TC_2), \cos(TC_2)]$. $rad(\Delta TC_2)$ represents the radian of ΔTC_2. By aligning timestamps of two CA paths, a path with five linear phases are obtained: $\{P_{1\_0} - P_{1\_1}, P_{1\_1} - P_{1\_2}, P_{1\_2} - P_{1\_3}, P_{1\_3} - P_{1\_4}, P_{1\_4} - P_{1\_5}\}$ for S_1 and $\{P_{2\_0} - P_{2\_1}, P_{2\_1} - P_{2\_2}, P_{2\_2} - P_{2\_3}, P_{2\_3} - P_{2\_4}, P_{2\_4} - P_{2\_5}\}$ for S_2.

The DDV to indicate conflict risk in the phase t_u and t_{u+1} is calculated as follows

$$DDV(u, u+1) = \begin{cases} DDV(u), TDV_1 < t_u \\ DDV, t_u \le TDV_1 < t_{u+1} \\ DDV(u+1), t_{u+1} \le TDV_1 \end{cases} \tag{13}$$

where TDV_1 is time to domain violation through Eq. (2).

Calculating all *DDV*s of two phases within the same time, the conflict risk function for *Ship* S_i in five phases is

$$f_i(DDV) = \max\{DDV(u, u+1) | u = 0, 1, 2, 3, 4\} \tag{14}$$

The conflict risk with n ships in the cluster is

$$f_{risk} = \max\{f_i(DDV) | i = 1, 2, 3, \ldots, n\} \tag{15}$$

3.2.2.2. Constraints. From the perspective of the CA process, the ship action time t_a should be earlier than the minimum TDV_1 of other ships in the cluster to avoid domain invasion of other ships. Besides, the action time is later than the beginning time of interference t_b in the cluster, which is to avoid affecting other ships outside the cluster. Thus, the ship action time t_a follows the condition:

$$t_b \le t_a \le \min TDV_1 \tag{16}$$

Considering the maneuvering feasibility, the constraints for course alteration are

$$\Delta TC = \begin{cases} (0, 90), \text{only conflicts in head} - \text{on situation} \\ (-90, 90), \text{other situations} \end{cases} \tag{17}$$

Regarding the other parameters, the maximum deviating distance for CA path options f_{Dev} in the cluster should be smaller than D_{CA} of the spatial cluster parameter. This precaution is taken to avoid potential collision risk with other ships situated outside the designated cluster.

$$f_{Dev} = \left[v \cdot t_r + 2R_s \cdot \tan\frac{\Delta TC}{2} - R_s \cdot rad(\Delta TC) \right] \cdot \sin\Delta TC \tag{18}$$

$$\max(f_{Dev}) \le D_{CA} \tag{19}$$

Finally, the conflict risk in the cluster should be smaller than the risk threshold value f_0 to reserve a safety margin.

$$f_{risk} \le f_0 \tag{20}$$

3.2.2.3. Objective function. In this research, the voyage loss is used as the objective function for optimization, which refers to the difference between the planned CA path and the actual path. It minimizes the loss from the global path viewpoint, which brings the ship back to the initial course as soon as feasible.

$$f_{loss} = v \cdot t_r + R_s \cdot rad(\Delta TC) - \left[v \cdot t_r + 2R_s \cdot \tan\frac{\Delta TC}{2} + R_s \cdot rad(\Delta TC) \right] \cdot \cos\Delta TC \tag{21}$$

3.2.2.4. Optimization solution algorithm. The PSO algorithm is adopted in this research to solve the optimization problem. The overall idea is:

$$\mathrm{P}: \begin{cases} \min f_{loss} \\ \text{subject to}: (16) - (20) \end{cases} \tag{22}$$

where the objective function is defined in Eq. (21) and the variables refer to $[t_a, \Delta TC, t_r]$.

3.2.3. Coordinated CA decisions within clusters

Under the methodology of distributed search (Kim et al., 2014), in each round of collaboration, one ship is allowed to initiate its CA action only after the other ship's action has been executed, and it has stabilized on its new course. However, this approach may not accurately reflect the actions of ships in busy waters. In light of this, an enhanced distributed coordination strategy is introduced in this paper to explore optimal solutions within ship clusters. The steps are as follows:

Step 1 : Ship Si within one conflict cluster exchanges her sailing state and action intention with other ships in the same cluster, including the current position, course, speed, and the planned CA option $Path_k$.

Step 2 : Ship Si obtains her optimal CA path $Path_k'$ by PSO solution algorithms using the received sailing information from other ships.

Step 3 : The planned path $Path_k$ and the optimal CA path $Path_k'$ of Ship Si are exchanged. The conflict improvement function $f_{impv}(Path_k')$ is presented in Eq. (23), which is calculated within the conflict clusters. Based on the results, the ship with the largest value of $f_{impv}(Path_{ki}')$ is determined as the action ship with top priority.

Step 4 : The planned CA option $Path_{ki}$ for the action ship with top priority is replaced by the optimal CA path $Path_{ki}'$.

Step 5 : If there still exists direct conflicts or potential CA conflicts with other ships in the cluster after taking the CA option $Path_k$, steps 2 to 5 are repeated until all conflicts are eliminated.

$$f_{impv}(Path_{ki}^{'}) = \frac{\sum_{j=1,i\neq j}^{n} f_{risk}(Path_i, Path_j) - \sum_{j=1,i\neq j}^{n} f_{risk}(Path_i^{'}, Path_j^{'})}{\sum_{j=1,i\neq j}^{n} f_{risk}(Path_i, Path_j)} + \left(\exp\left(\frac{\max(\beta - TDV_{k\_\min}, 0)}{\alpha}\right) - 1\right) \quad (23)$$

where n is the total number of ships in the cluster; $f_{risk}(Path_i, Path_j)$ is the collision risk between the planned CA options $Path_i$ of *Ship* S_i and the planned CA options $Path_j$ of *Ship* S_j; $f_{risk}(Path_i^{'}, Path_j)$ is the collision risk between the optimal CA option $Path_i^{'}$ and the planned path option $Path_j$ of *Ship* S_j; $TDV_{i\_\min}$ is the minimum *TDV* of *Ship* S_i concerning other ships in the cluster; β is the temporal thresholds determined by temporal collision hazard, typically 12 min; α defaults as $6/\ln 2$ to increase the improvement by 1 when $TDV_{i\_\min}$ reaches 6 min.

3.3. Conflict cluster update

In each round of conflict detection, a ship can exclusively participate in a single cluster to formulate CA decisions and execute corresponding actions. During the full process of a multi-ship encounter, the composition of the clusters undergoes constant modifications, wherein certain ships might exit one cluster and potentially join another. The dissolution of a cluster occurs when the ships within it meet any of the following conditions.

(1) All ships taking CA actions in the cluster have recovered their initial course and become stable on the course.
(2) The ships maintaining their course and speed will not cause any direct conflict or potential CA conflict with other ships in the same cluster.
(3) All ships in the clusters will not cause any direct conflict or potential CA conflict with each other.

Once any of the above conditions are fulfilled, the subsequent round of conflict cluster detection will be activated for all involved ships using the conflict cluster detection model in Section 3.1.

4. Simulation and discussions

To test the proposed CA decision-making method based on conflict cluster detection, a simulation experiment is performed, and the result is compared to other methods. Simulation tests are conducted on the MATLAB® software platform, utilizing an i5-13500H CPU and 16 GB RAM. A specific model for a general cargo ship is employed to simulate the ship's movements, as described by (Zhang et al., 2015). The simulations assumed that all ships in the scenario are equipped with AIS and other communication systems, enabling them to broadcast and update their dynamic information and planned paths with a satisfactory frequency. The ship domain radius is defined as six times the length of the ship. The setup of the simulation scenario is introduced in Section 4.1, with the results by conflict cluster-based approach and other methods in Section 4.2 and Section 4.3, respectively. Section 4.4 compares and discusses the results.

4.1. Scenario setup

To present the effectiveness of the proposed method, a multi-ship encounter involving 11 ships is taken as the simulation scenario, as shown in Fig. 12. The detailed position, course, and speed of the ships are listed in Table 2.

4.2. Conflict cluster-based simulation results

Applying the proposed conflict cluster detection method, the simulation results of the conflict cluster-based CA decision-making is elaborated as follows.

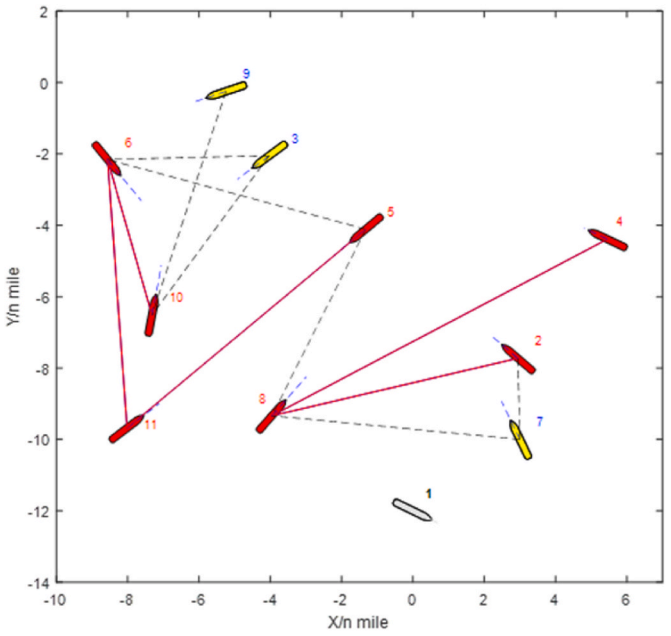

Fig. 12. The simulation scenario with 11 ships in a multi-ship encounter situation.. (The solid red lines link the ships with a direct conflict, and the dotted blue lines link the ships with a potential CA conflict.)

Table 2
The initial status of 11 ships in the encounter situation.

Ship No.	Position (n mile)		Course (°)	Speed (kn)
	X	Y		
s_1	0.0	−12.0	116	9.1
s_2	2.9	−7.7	311	11.3
s_3	−4.0	−2.1	234	13.3
s_4	5.5	−4.4	295	8.6
s_5	−1.3	−4.1	230	11.7
s_6	−8.6	−2.2	141	18.0
s_7	3.0	−10.0	334	14.3
s_8	−4.0	−9.3	41	17.5
s_9	−5.2	−0.2	251	10.7
s_{10}	−7.3	−6.5	11	17.0
s_{11}	−8.1	−9.8	51	11.0

4.2.1. Preliminary hierarchical clustering

Representing 11 ships by $S = \{s_1, s_2, \ldots, s_{11}\}$, the variable C describes the ship pairs with either a direct conflict or a potential CA conflict by the value *TWC* for each ship pair, including 12 ship pairs:

$$C = \left\{TWC_{2\_7}, TWC_{2\_8}, TWC_{3\_6}, \ldots, TWC_{7\_8}, TWC_{9\_10}\right\} \quad (24)$$

Taking the ship pair (s_2, s_7) with a direct conflict as an example, according to the calculation of encounter parameters in Section 3.1.1, TWC_{2_7} can be calculated as $t_b = 0$ and $t_e = 34.8$ min. For the ship pair (s_7, s_8) with a potential CA conflict, TWC_{7_8} can also be calculated: $t_b^{'} = 24.2$ min and $t_e^{'} = 28.2$ min.

The similarity matrix E between 12 ship pairs is calculated by Eq. (9):

$$E = \begin{bmatrix} 0 & 0 & \ldots & 0 & \text{inf} \\ 0 & 0 & \ldots & 1.1 & \text{inf} \\ \vdots & \vdots & \cdots & \vdots & \vdots \\ 0 & 1.1 & \ldots & 0 & \text{inf} \\ \text{inf} & \text{inf} & \ldots & \text{inf} & 0 \end{bmatrix}_{12\times 12} \quad (25)$$

where $E(11,2) = dis(pair(s_7, s_8), pair(s_2, s_8)) = C(1,11) - C(2,2) = 24.6 - 23.5 = 1.1$ min.

The matrix is further simplified to a binary-tree-like hierarchical index matrix:

$$E\_bt = \begin{bmatrix} 2 & 1 & 0 \\ 4 & 3 & 0 \\ \vdots & \vdots & \vdots \\ 22 & 12 & 1.3 \end{bmatrix}_{11\times 3} \tag{26}$$

where $E\_bt(:, 1:2)$ indicates binary-tree-like indexes of the ship pair; $E\_bt(:, 3)$ refers to the similarity between two ship pairs, explained on lines 7–8 in **Algorithm 1**.

Preliminarily, the ships are clustered as $\varsigma_{in}^{1} = \{s_2, s_3, s_4, s_5, s_6, s_7, s_8, s_9, s_{10}, s_{11}\}$ and $\varsigma_{out} = \{s_1\}$ according to line 12 in **Algorithm 1**, as shown in Fig. 13.

4.2.2. Final cluster determination

The number of ships in each cluster can be finally determined by adjusting the clustering parameters. In this case, the maximum number of ships in one cluster is limited to five ships. Therefore, the ships in preliminary cluster G_1 are divided into two clusters $G_1 = \{s_2, s_4, s_7, s_8\}$ and $G_2 = \{s_3, s_5, s_6, s_{10}, s_{11}\}$ by adjusting the parameters from $D_{CA} = 1.5$ n mile, $t_b = 0$, and $t_c = 5$ min to $D_{CA} = 1.3$ n mile, $t_b = 1$ min, and $t_c = 3$ min, with $C_{final} = \begin{bmatrix} 4.9 & 5.0 & \dots & 24.2 & 16.5 \\ 29.4 & 22.7 & \dots & 26.8 & 17.7 \end{bmatrix}_{2\times 11}$, $E\_bt_{final} = \begin{bmatrix} 2 & 1 & 0 \\ 4 & 3 & 0 \\ \vdots & \vdots & \vdots \\ 11 & 19 & 3.2 \\ 14 & 20 & \text{inf} \end{bmatrix}_{10\times 3}$.

The adjusted clustering result is presented in Fig. 14. It can be found that the preliminary cluster is divided into two clusters due to the potential CA conflict between s_5 and s_8. At the same time, *Ship* s_9 is excluded from the clusters, since the distance between $pair(s_9, s_{10})$ and $pair(s_3, s_{10})$ is 3.2 min, which is larger than the threshold $t_c = 3$ min.

4.2.3. CA decision-making

In each round of conflict resolution, the action ship and the corresponding CA decisions with the actions are determined according to the maximum conflict improvement f_{impv}, as listed in Table 3. Taking $G_2 = \{s_3, s_5, s_6, s_{10}, s_{11}\}$ as an example, in the first round, five ships independently search for their optional CA decisions according to the conflict resolution algorithm, being $(Path_3', Path_5', Path_6', Path_{10}', Path_{11}')$. According to the results, $Path_{11}'$ for *Ship* s_{11}, [1.7, 16, 13.0] means the ship will take a course alteration of 16° to the starboard side at 1.7 min and recover the original path at 14.7 min. Such a CA decision leads to the biggest conflict improvement of 1.82. Thus, *Ship* s_{11} is determined as the action ship for this round of decision-making. Afterwards, $Path_{11}'$ replaces the planned path $Path_{11}$ [0, 0, 0] to exchange sailing information. After two rounds of coordinated CA decision resolution, the final CA decision for this cluster involving five ships can be obtained $\begin{bmatrix} 0.0 & 0.0 & 0.0 \\ 0.0 & 0.0 & 0.0 \\ 1.0 & 24 & 5.4 \\ 0.0 & 0.0 & 0.0 \\ 1.7 & 16 & 13.0 \end{bmatrix}$. In the results, $[0.0 \quad 0.0 \quad 0.0]$ means ships s_3, s_5, and s_{10} shall maintain their current course and speed from the current time till the ending time of the cluster.

Similarly, the CA decisions for ships in $G_1 = \{s_2, s_4, s_7, s_8\}$ can be obtained. The CA decisions for two clusters of ships are listed in Table 4. The corresponding ships will take action in a coordinated way.

To illustrate simulation results, the ship positions and their trajectories at four typical time stamps are presented in Fig. 15: (1) time = 0 min (initial time, two clusters); (2) time = 14 min (*Ship* s_8 just recovers her course); (3) time = 18 min (all ships just meet the condition of reclustering); (4) time = 32 min (all ships have completed their CA actions and all conflict clusters are dissolved).

Taking cluster G_1 as an example, *Ship* s_8 will take a course alteration of 20° to port side at 1.3 min and recover the original course at 13.7 min. It is estimated that s_8 will pass other ships well clear at 16.6 min, which fulfils reclustering condition. At the same time, cluster G_1 will be dissolved since no conflict risk exists in the cluster anymore. Thus, all ships s_2, s_4, s_7, and s_8 join $\mathscr{S}_{out}$. The distance between any pair of two ships during the entire CA process in the 11-ship encounter is shown in Fig. 16. The results show that all involved ships pass each other well clear with a minimum distance of 0.69 n mile for $pair(s_3, s_{10})$, followed by 0.75 n mile for $pair(s_6, s_{10})$, due to the CA action by *Ship* s_6 at a safety margin.

4.3. Simulation results with non-cluster methods

For the above-mentioned simulation scenario of an 11-ship encounter, three non-cluster CA decision-making methods are tested for comparison: (1) DDV/TDV-based coordinated CA method; (2) global coordinated CA method; (3) distributed CA method.

4.3.1. DDV/TDV-based coordinated CA method

In the DDV/TDV-based coordinated CA method, once the condition of a direct conflict is fulfilled, the ships will take coordinated CA actions based on the CA decision-making and coordination strategy as stated in Section 3.2. The CA trajectories and the distance between any pair of two ships during the entire process are shown in Fig. 17. During the process, the minimum distance between ships is 0.69 n mile for $pair(s_3, s_{10})$, followed by 0.70 n mile for $pair(s_7, s_8)$, due to the action by *Ship* s_8 at safety margin. The CA actions by ships s_8, s_6, s_5, and s_{11} refer to 30

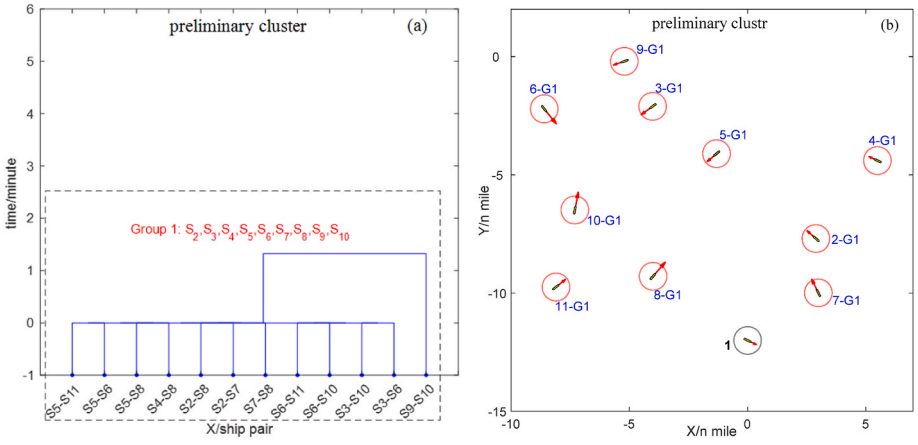

Fig. 13. Preliminary clustering results: (a) hierarchical tree diagram; (b) corresponding position of the ships in clusters.

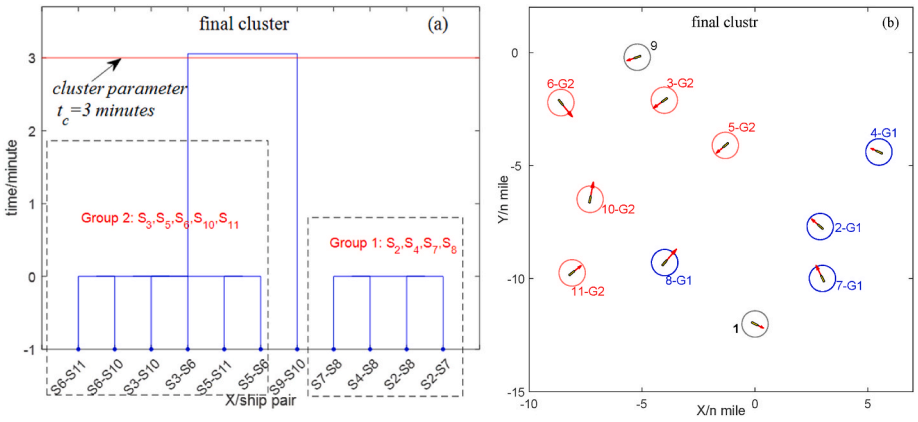

Fig. 14. Adjusted clustering results: (a) hierarchical tree diagram; (b) corresponding position of the ships in clusters.

Table 3
Coordinated CA decision-making process within clusters.

Round No.	Conflict improvement f_{impv}	Action ship	CA decision
1	[0.00,1.47,1.74,1.23,1.82]	s_{11}	[1.7,16,13.0]
2	[0.00,1.44,1.51,1.25,0.00]	s_6	[1.0,24,5.4]

Table 4
CA decisions for ships in clusters.

Cluster No.	Ship	CA decision			Time to meet the conditions of reclustering
		t_a (minute)	ΔTC (°)	t_r (minute)	
G_1	s_2	–	–	–	16.6
	s_4	–	–	–	16.6
	s_7	–	–	–	16.6
	s_8	1.3	−20	12.4	16.6
G_2	s_3	–	–	–	17.6
	s_5	–	–	–	17.6
	s_6	1.0	24	5.4	17.6
	s_{10}	–	–	–	17.0
	s_{11}	1.7	16	13.0	17.6

degrees of starboard course alteration at 1 min, 29 degrees of starboard course alteration at 1 min, 17 degrees of starboard course alteration at 1 min, and 18 degrees of starboard course alteration at 2 min, respectively. *Ship* s_8 detects new collision risk with s_7 at 12 min, and turns starboard by 28° at 13 min, while the potential CA conflict with *Ship* s_7 is ignored.

4.3.2. Global coordinated CA method

The global coordinated CA method is expected to generate coordinated actions for all ships in multi-ship encounter situations. Taking the CA decision-making and coordination strategy in Section 3.2, the CA trajectories and the distance between any pair of two ships during the entire process are shown in Fig. 18. Specifically, ships *s*5, *s*6, and *s*8 take CA actions involving 9 degrees of starboard course alteration at 1 min, 22 degrees of starboard course alteration at 2 min, and 10 degrees of portside course alteration at 5 min, respectively. From the viewpoint of CA effects, the minimum distance for $pair(s_3, s_{10})$ is 0.69 n mile, followed by 0.72 n mile for $pair(s_4, s_8)$, due to the CA action by *Ship* s_8 with a safety margin.

4.3.3. Distributed CA method

In the distributed CA method, each ship makes CA decisions to keep the clearance of all other ships from the perspective of own ship. These individual ship actions are expected to solve the collision conflict. However, it may cause uncoordinated actions between ships due to a lack of CA intentions exchange, which is a typical non-cooperative CA method. When a collision risk is triggered ($0 < DDV$ and $0 < TDV_2 < 30$ min), each involved ship takes CA action to solve the problem. The ship trajectories are presented in Fig. 19, with a minimum distance of 0.45 n mile for the $pair(s_3, s_{10})$ after seven ships taking CA actions. In addition, it can be observed that each ship takes a series of frequent course alterations, which leads to a long sailing track.

4.4. Comparison and discussions

The simulation results of the proposed cluster-based method and the three non-cluster methods are compared from the perspectives of safety, economy, and computational loads. Several indicators are selected, including the minimum distance between pairs of ships, the maximum and total deviating distance, the number of ships in action, the quantity of CA actions taken, and the number of calls to the solution algorithm. The comparison results are listed in Table 5.

From a safety perspective, both the cluster-based and non-cluster CA methods can effectively prevent collisions. Adopting coordinated CA, the cluster-based approach and the two non-cluster methods provide decisions at a minimum distance of 0.69 n miles. The non-cluster with distributed CA method contributes to a safety distance of 0.45 n miles between s_3 and s_{10}. The difference arises from the opposite course alteration executed by the distributed CA method when *Ship* s_3 changes its course to portside to avoid *Ship* s_6, while *Ship* s_{10} turns starboard to avoid *Ship* s_3.

From an economic viewpoint, the distributed CA method generates the largest deviation distance, as the decision-making of all ships is constantly influenced by the CA actions of any involved ship. On the contrary, the globally coordinated CA method results in the minimum deviation distance with the fewest number of actions because of the collaboration among all involved ships. However, the DDV/TDV-based coordinated CA method requires four times more CA actions due to the potential conflict caused by *Ship* s_7, as depicted in Fig. 17. It implies that both direct conflicts and potential conflicts are considered. Comparing the deviation distances, the result from the cluster-based method is larger than the globally coordinated method, but the same in the numbers of action ships and actions.

In terms of computation load, the number of calls to the solution algorithm is an essential cost, especially for non-linear optimization problems. The distributed CA method solely executes a one-time solution algorithm to generate temporary CA decision. In the results, the global coordinated method requires 38 runs to achieve collaboration among all ships, followed by 14 runs by the DDV/TDV-based method. However, the proposed method bears the smallest computation load as it conducts CA coordination within ship clusters, which significantly reduces the necessary number of optimization algorithm calls.

In summary, the proposed method considers both the conflict con-

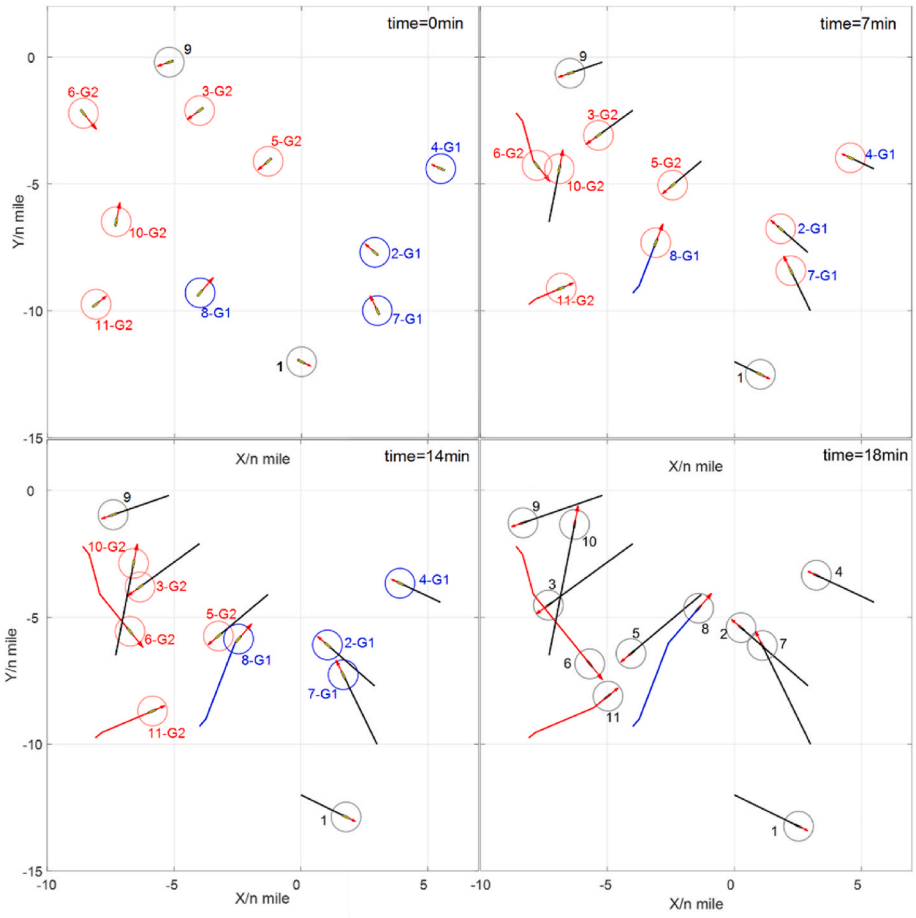

Fig. 15. The position of ships with the changing composition of clusters during the CA process in the 11-ship encounter scenario.. (Ships marked by gray numbers represent ships outside the conflict clusters, while ships marked in blue number represent the ones in conflict clusters, e.g., 2-G1 means s_2 in conflict cluster G_1.)

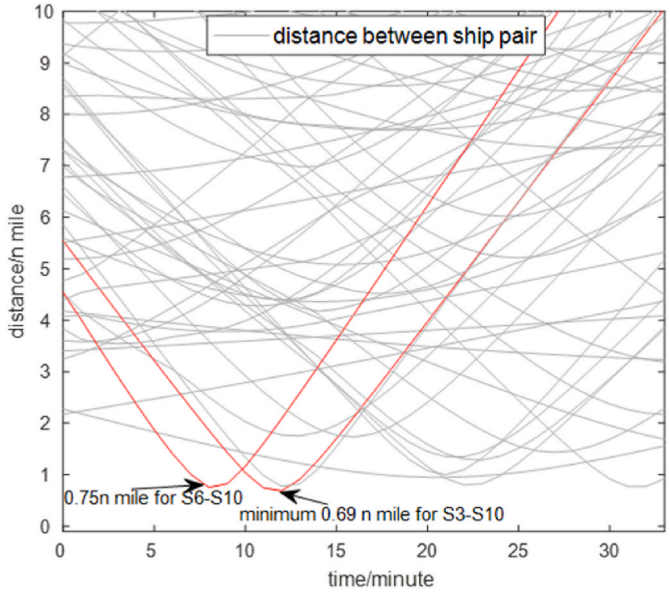

Fig. 16. The distance between any pair of two ships during the CA process in the encounter scenario.

nectivity and the spatiotemporal interactions during CA actions by *DDV*, *TDV*, and *TWC* throughout the entire process of multi-ship encounters. It effectively identifies direct conflicts and potential CA conflicts ascribed to the CA actions by any involved ship. The results reveal a comprehensive balance between safety and economy concerns, as well as the computational load issue. Such a balance also meets the requirement in navigational practice. Particularly in busy waters with numerous ships within a limited area, the computation load by the global coordination method increases significantly. The number of CA actions by the DDV/TDV-based coordination method is expected to increase when more potential CA conflicts exist, such as *Ship* s_7 in Fig. 17. Therefore, in busy waters with frequent multi-ship encounters, the proposed method provides coordinated CA decisions with a feasible computation load, which is practical for officers on board and VTS operators.

4.5. Potential limitations and further improvements

Although the proposed method provides satisfactory CA suggestions according to the simulation results, there still exist some potential limitations. Firstly, regarding the design of the ship domain model, more influencing factors can be incorporated. In this research, the ship safety domain is simplified as a circular shape. However, the shape and size of the ship domain heavily depend on the characteristics of involved ships, local traffic density, and traffic rules in the area. Therefore, in future studies, it is recommended to consider additional factors in designing the ship domain to provide more applicable CA suggestions in accord with the navigational practice. Secondly, the method to predict the trajectories of non-cooperative ships can be further extended. In this research, the proposed methodology relies on the assumption that all involved ships exchange information about their CA actions through communications. However, in navigational practice, some ships may not share their navigation plans because of their own subjective non-

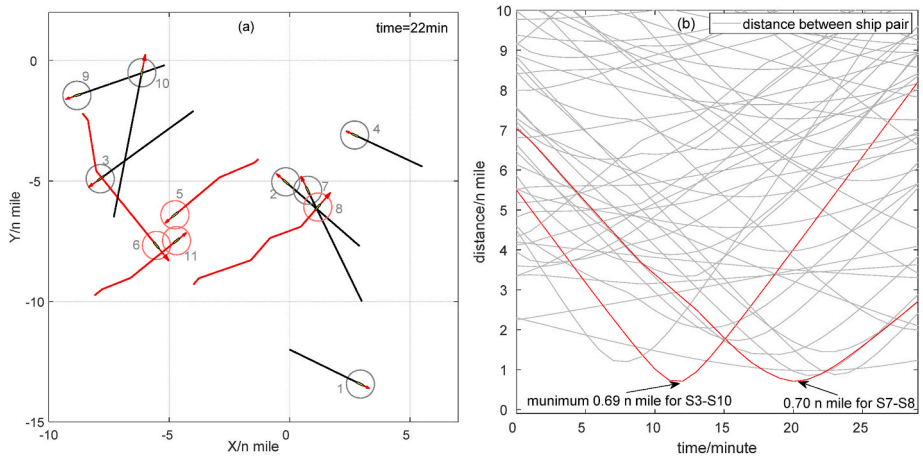

Fig. 17. The CA process during the 11-ships encounter scenario by DDV/TDV-based coordinated CA method. ((a) Coordinated CA trajectories at 22 min; (b) distance between any pair of two ships during the entire process.).

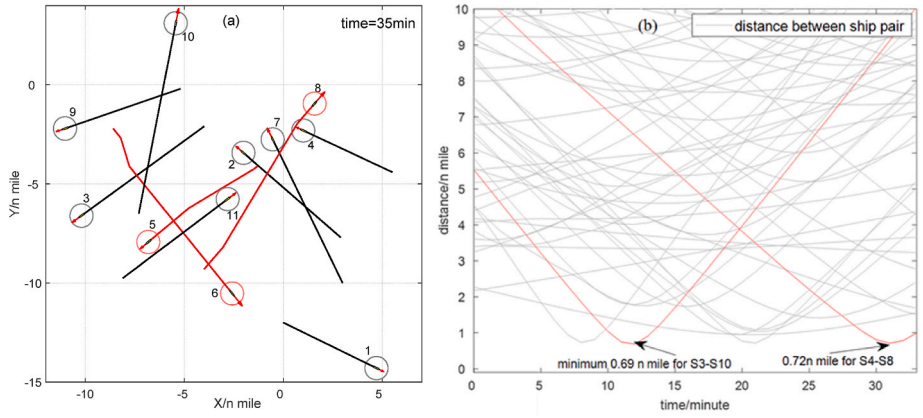

Fig. 18. The CA process during an 11-ship encounter scenario by the global coordinated CA method. ((a) Coordinated CA trajectories at 35 min; (b) distance between any pair of two ships during the entire process.).

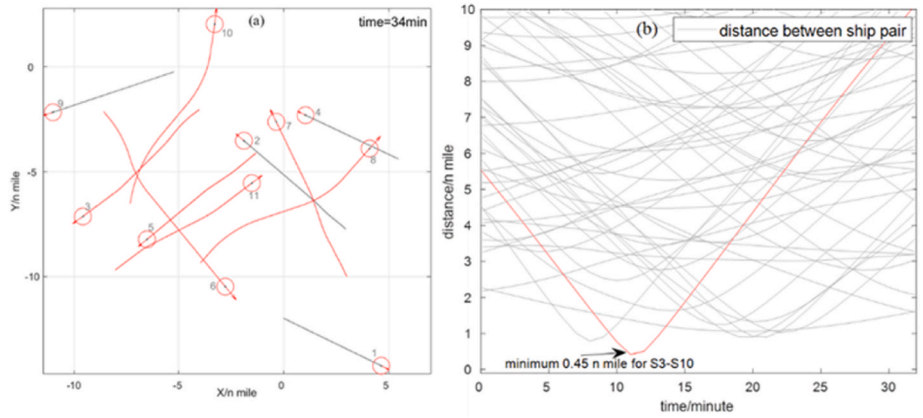

Fig. 19. The CA process during an 11-ship encounter scenario by distributed CA method. ((a) CA trajectories at 34 min; (b) distance between any pair of two ships during the entire process.).

cooperative reasons or objective equipment limitations. To address this issue, maneuver-based trajectory prediction techniques can be integrated into the model, which does not require information exchange as the premise. These prediction techniques will further support the conflict cluster-based CA decision-making for non-cooperative ships. Finally, in the case to avoid the immediate danger of collision, the ships must change both course and speed. Such CA actions should be included in future studies based on a distinguishing definition and assessment of collision risk and immediate danger.

Table 5
Comparison of the proposed cluster-based approach and non-cluster CA methods.

Method		Minimum distance (n mile)	Deviating distance (n mile)		No. of action ships	No. of CA actions	No. of solution algorithm calls
			max	sum			
Cluster	**Cluster-based approach**	**0.69**	**1.28**	**2.89**	**3**	**3**	**13**
Non-cluster	DDV/TDV-based coordinated CA	0.69	1.19	3.85	4	5	14
	Global coordinated CA	0.69	1.18	2.43	3	3	38
	Distributed CA	0.45	3.3	13.6	7	>7	–

5. Conclusions

In this research, a conflict cluster-based method for coordinated CA decision-making in multi-ship encounters is proposed. From a theoretical perspective, the proposed method can effectively identify the conflict clusters by considering both the direct conflict connectivity and the potential spatiotemporal interactions due to the planned CA actions. When integrated into the CA decision-making process within the proposed framework, this method can generate stable clusters with CA actions during the entire encounter process.

Taking an 11-ship encounter situation as the simulation scenario, the effectiveness of the proposed conflict cluster-based approach is demonstrated. The results show that all involved ships are capable of executing efficient and coordinated CA actions. By comparing the simulation results with non-cluster methods, the cluster-based method can provide feasible CA decisions with reduced deviating distance and a lower computation load. From both safety and economic perspectives, the proposed method proves its practicality in real-life navigation.

CRediT authorship contribution statement

Kezhong Liu: Conceptualization, Supervision, Funding acquisition. **Xiaolie Wu:** Methodology, Formal analysis, Investigation, Writing – original draft, Writing – review & editing. **Yang Zhou:** Supervision, Writing – original draft, Writing – review & editing. **Zhitao Yuan:** Investigation. **Xing Yang:** Supervision, Investigation. **Xuri Xin:** Methodology. **Sujie Zhuang:** Methodology.

Declaration of competing interest

The authors declare that they have no known competing financial interests or personal relationships that could have appeared to influence the work reported in this paper.

Data availability

No data was used for the research described in the article.

Acknowledgement

This research was funded by National Natural Science Foundation of China (Grant No. 52031009).

List of symbols

Symbols	*Definitions*
R_d	Ship domain radius
DDV	Degrees of violating the domain
TDV_1	Time of violating the domain
TDV_2	Time of leaving the domain
t_0	Current time
t_b	Beginning time of a direct conflict
t_e	Ending time of a direct conflict
$t_b^{'}$	Beginning time of a potential CA conflict
$t_e^{'}$	Ending time of a potential CA conflict
TWC	Time window of conflict
dis	Distance between ship pairs with conflicts
D_{CA}	Deviating distance for CA actions
t_c	Time for the ships being past and clear
t_a	Time of CA actions
ΔTC	Magnitude of course alteration
t_r	Time to recover the original course
R_s	Maneuvering radius of course alteration

References

Akdağ, M., Solnør, P., Johansen, T.A., 2022. Collaborative collision avoidance for maritime autonomous surface ships: a review. Ocean Eng 250, 110920.

Bakdi, A., Glad, I.K., Vanem, E., 2021. Testbed scenario design exploiting traffic big data for autonomous ship trials under multiple conflicts with collision/grounding risks and spatiooral dependencies. IEEE Trans. Intell. Transport. Syst. 22, 7914–7930. https://doi.org/10.1109/TITS.2021.3095547.

Chen, P., Huang, Y., Mou, J., Gelder, P.H.A., 2019. Probabilistic risk analysis for ship-ship collision : state-of-the-art. Saf. Sci. 117, 108–122. https://doi.org/10.1016/j.ssci.2019.04.014.

Chen, P., Huang, Y., Mou, J., van Gelder, P., 2018. Ship collision candidate detection method: a velocity obstacle approach. Ocean Eng. 170, 186–198.

Chen, P., Huang, Y., Papadimitriou, E., Mou, J., van Gelder, P., 2020. An improved time discretized non-linear velocity obstacle method for multi-ship encounter detection. Ocean Eng. 196, 106718.

Cho, Y., Han, J., Kim, J., 2020. Efficient COLREG-compliant collision avoidance in multi-ship encounter situations. IEEE Trans. Intell. Transport. Syst. 1–13. https://doi.org/10.1109/tits.2020.3029279.

Dinh, G.H., Im, N.-K., 2016. The combination of analytical and statistical method to define polygonal ship domain and reflect human experiences in estimating dangerous area. Int. J. e-Navigation Marit. Econ. 4, 97–108.
Du, L., Banda, O.A.V., Huang, Y., Goerlandt, F., Kujala, P., Zhang, W., 2021. An empirical ship domain based on evasive maneuver and perceived collision risk. Reliab. Eng. Syst. Saf. 213, 107752.
Fujii, Y., Tanaka, K., 1971. Traffic capacity. J. Navig. 24, 543–552.
Gil, M., Kozioł, P., Wróbel, K., Montewka, J., 2022. Know your safety indicator–A determination of merchant vessels Bow Crossing Range based on big data analytics. Reliab. Eng. Syst. Saf. 220, 108311.
Gil, M., Montewka, J., Krata, P., Hinz, T., Hirdaris, S., 2020. Determination of the Dynamic Critical Maneuvering Area in an Encounter between Two Vessels.
Goerlandt, F., Montewka, J., Lammi, H., Kujala, P., 2012. Analysis of near collisions in the Gulf of Finland. Adv. Safety, Reliab. Risk Manag. 2880–2886.
He, Y., Jin, Y., Huang, L., Xiong, Y., Chen, P., Mou, J., 2017. Quantitative analysis of COLREG rules and seamanship for autonomous collision avoidance at open sea. Ocean Eng. 140, 281–291. https://doi.org/10.1016/j.oceaneng.2017.05.029.
Hu, L., Naeem, W., Rajabally, E., Watson, G., Mills, T., Bhuiyan, Z., Raeburn, C., Salter, I., Pekcan, C., 2020. A multiobjective optimization approach for COLREGs-Compliant path planning of autonomous surface vehicles verified on networked bridge simulators. IEEE Trans. Intell. Transport. Syst. 21, 1167–1179. https://doi.org/10.1109/TITS.2019.2902927.
Hu, L., Naeem, W., Rajabally, E., Watson, G., Mills, T., Bhuiyan, Z., Raeburn, C., Salter, I., Pekcan, C., 2019. A multiobjective optimization approach for COLREGs-compliant path planning of autonomous surface vehicles verified on networked bridge simulators. IEEE Trans. Intell. Transport. Syst. 21, 1167–1179.
Huang, Y., Chen, L., Chen, P., Negenborn, R.R., van Gelder, P.H.A.J.M., 2020. Ship collision avoidance methods: state-of-the-art. Saf. Sci. 121, 451–473. https://doi.org/10.1016/j.ssci.2019.09.018.
Huang, Y., Chen, L., van Gelder, P.H.A.J.M., 2019. Generalized velocity obstacle algorithm for preventing ship collisions at sea. Ocean Eng. 173, 142–156. https://doi.org/10.1016/j.oceaneng.2018.12.053.
Johansen, T.A., Perez, T., Cristofaro, A., 2016. Ship collision avoidance and COLREGS compliance using simulation-based control behavior selection with predictive hazard assessment. IEEE Trans. Intell. Transport. Syst. 17, 3407–3422. https://doi.org/10.1109/TITS.2016.2551780.
Kang, Y.-T., Chen, W.-J., Zhu, D.-Q., Wang, J.-H., Xie, Q.-M., 2018. Collision avoidance path planning for ships by particle swarm optimization. J. Mar. Sci. Technol. 26, 3.
Kim, D.-G., Hirayama, K., Park, G.-K., 2014. Collision avoidance in multiple-ship situations by distributed local search. J. Adv. Comput. Intell. Intell. Inf. 18, 839–848.
Kim, D., Hirayama, K., Okimoto, T., 2017. Distributed stochastic search algorithm for multi-ship encounter situations. J. Navig. 70, 699–718.
Kulkarni, K., Goerlandt, F., Li, J., Banda, O.V., Kujala, P., 2020. Preventing shipping accidents: past, present, and future of waterway risk management with Baltic Sea focus. Saf. Sci. 129, 104798.
Kundakçı, B., Nas, S., Gucma, L., 2023. Prediction of ship domain on coastal waters by using AIS data. Ocean Eng. 273, 113921.
Lazarowska, A., 2015. Ship's trajectory planning for collision avoidance at sea based on ant colony optimisation. J. Navig. 68, 291–307.
Li, J., Wang, H., Guan, Z., Pan, C., 2020. Distributed multi-objective algorithm for preventing multi-ship collisions at Sea. J. Navig. 73, 971–990. https://doi.org/10.1017/S0373463320000053.
Li, M., Mou, J., Chen, L., He, Y., Huang, Y., 2021. A rule-aware time-varying conflict risk measure for MASS considering maritime practice. Reliab. Eng. Syst. Saf. 215, 107816.
Li, M., Mou, J., Chen, P., Rong, H., Chen, L., van Gelder, P., 2022. Towards real-time ship collision risk analysis: an improved R-TCR model considering target ship motion uncertainty. Reliab. Eng. Syst. Saf. 226, 108650.
Li, S., Liu, J., Negenborn, R.R., 2019. Distributed coordination for collision avoidance of multiple ships considering ship maneuverability. Ocean Eng. 181, 212–226. https://doi.org/10.1016/j.oceaneng.2019.03.054.
Liu, J., Zhang, J., Yan, X., Soares, C.G., 2022. Multi-ship collision avoidance decision-making and coordination mechanism in Mixed Navigation Scenarios. Ocean Eng. 257, 111666.
Liu, J., Zhou, F., Li, Z., Wang, M., Liu, R.W., 2016. Dynamic ship domain models for capacity analysis of restricted water channels. J. Navig. 69, 481–503.
Liu, R.W., Liang, M., Nie, J., Yuan, Y., Xiong, Z., Yu, H., Guizani, N., 2022. STMGCN: mobile edge computing-empowered vessel trajectory prediction using spatio-temporal multigraph convolutional network. IEEE Trans. Ind. Inf. 18, 7977–7987.
Liu, Y., Liu, W., Song, R., Bucknall, R., 2017. Predictive navigation of unmanned surface vehicles in a dynamic maritime environment when using the fast marching method. Int. J. Adapt. Control Signal Process. 31, 464–488.
Lyu, H., Yin, Y., 2019. COLREGS-constrained real-time path planning for autonomous ships using modified artificial potential fields. J. Navig. 72, 588–608. https://doi.org/10.1017/S0373463318000796.
Mou, J., Li, M., Hu, W., Zhang, X., Gong, S., Chen, P., He, Y., 2021. Mechanism of dynamic automatic collision avoidance and the optimal route in multi-ship encounter situations. J. Mar. Sci. Technol. 26, 141–158. https://doi.org/10.1007/s00773-020-00727-4.
Park, J., Choi, J., Choi, H.T., 2019. COLREGS-compliant path planning considering time-varying trajectory uncertainty of autonomous surface vehicle. Electron. Lett. 55, 222–224. https://doi.org/10.1049/el.2018.6680.
Park, J., Kim, J., 2016. Predictive evaluation of ship collision risk using the concept of probability flow. IEEE J. Ocean. Eng. 42, 836–845.
Perera, L.P., Carvalho, J.P., Guedes Soares, C., 2011. Fuzzy logic based decision making system for collision avoidance of ocean navigation under critical collision conditions. J. Mar. Sci. Technol. 16, 84–99. https://doi.org/10.1007/s00773-010-0106-x.
Qu, X., Meng, Q., Suyi, L., 2011. Ship collision risk assessment for the Singapore Strait. Accid. Anal. Prev. 43, 2030–2036.
Rawson, A., Brito, M., 2021. A critique of the use of domain analysis for spatial collision risk assessment. Ocean Eng. 219, 108259.
Rong, H., Teixeira, A.P., Soares, C.G., 2022. Maritime traffic probabilistic prediction based on ship motion pattern extraction. Reliab. Eng. Syst. Saf. 217, 108061.
Shen, H., Hashimoto, H., Matsuda, A., Taniguchi, Y., Terada, D., Guo, C., 2019. Automatic collision avoidance of multiple ships based on deep Q-learning. Appl. Ocean Res. 86, 268–288. https://doi.org/10.1016/j.apor.2019.02.020.
Shi, Z., Zhen, R., Liu, J., 2022. Fuzzy logic-based modeling method for regional multi-ship collision risk assessment considering impacts of ship crossing angle and navigational environment. Ocean Eng. 259, 111847.
Szlapczynski, R., 2011. Evolutionary sets of safe ship trajectories: a new approach to collision avoidance. J. Navig. 64, 169–181.
Szlapczynski, R., Szlapczynska, J., 2016. An analysis of domain-based ship collision risk parameters. Ocean Eng. 126, 47–56.
Tam, C., Bucknall, R., 2013. Cooperative path planning algorithm for marine surface vessels. Ocean Eng. 57, 25–33.
Tsou, M.-C., 2016. Multi-target collision avoidance route planning under an ECDIS framework. Ocean Eng. 121, 268–278.
Vu, D.-T., Jeong, J.-Y., 2021. Collision risk assessment by using hierarchical clustering method and real-time data. J. Korean Soc. Mar. Environ. Saf. 27, 483–491.
Wang, N., 2013. A novel analytical framework for dynamic quaternion ship domains. J. Navig. 66, 265–281.
Wang, N., 2010. An intelligent spatial collision risk based on the quaternion ship domain. J. Navig. 63, 733–749.
Wang, T., Wu, Q., Zhang, J., Wu, B., Wang, Y., 2020. Autonomous decision-making scheme for multi-ship collision avoidance with iterative observation and inference. Ocean Eng. 197, 106873 https://doi.org/10.1016/j.oceaneng.2019.106873.
Wang, X., Liu, Z., Cai, Y., 2017. The ship maneuverability based collision avoidance dynamic support system in close-quarters situation. Ocean Eng. 146, 486–497.
Wang, Y., Chin, H.-C., 2016. An empirically-calibrated ship domain as a safety criterion for navigation in confined waters. J. Navig. 69, 257–276.
Woo, J., Kim, N., 2020. Collision avoidance for an unmanned surface vehicle using deep reinforcement learning. Ocean Eng. 199, 107001.
Xin, X., Liu, K., Loughney, S., Wang, J., Yang, Z., 2022. Maritime traffic clustering to capture high-risk multi-ship encounters in complex waters. Reliab. Eng. Syst. Saf., 108936
Xin, X., Liu, K., Yang, Z., Zhang, J., Wu, X., 2021. A probabilistic risk approach for the collision detection of multi-ships under spatiotemporal movement uncertainty. Reliab. Eng. Syst. Saf. 215, 107772 https://doi.org/10.1016/j.ress.2021.107772.
Xin, X., Yang, Z., Liu, K., Zhang, J., Wu, X., 2023. Multi-stage and multi-topology analysis of ship traffic complexity for probabilistic collision detection. Expert Syst. Appl. 213, 118890.
Yu, Q., Teixeira, A.P., Liu, K., Soares, C.G., 2022. Framework and application of multi-criteria ship collision risk assessment. Ocean Eng. 250, 111006.
Zhang, J., Zhang, D., Yan, X., Haugen, S., Guedes Soares, C., 2015. A distributed anti-collision decision support formulation in multi-ship encounter situations under COLREGs. Ocean Eng. 105, 336–348. https://doi.org/10.1016/j.oceaneng.2015.06.054.
Zhang, K., Huang, L., He, Y., Wang, B., Chen, J., Tian, Y., Zhao, X., 2023. A real-time multi-ship collision avoidance decision-making system for autonomous ships considering ship motion uncertainty. Ocean Eng. 278, 114205.
Zhang, W., Feng, X., Qi, Y., Shu, F., Zhang, Y., Wang, Y., 2019. Towards a model of regional vessel near-miss collision risk assessment for open waters based on AIS data. J. Navig. 72, 1449–1468.
Zhang, W., Goerlandt, F., Kujala, P., Wang, Y., 2016. An advanced method for detecting possible near miss ship collisions from AIS data. Ocean Eng. 124, 141–156.
Zhao, L., Roh, M.-I., 2019. COLREGs-compliant multiship collision avoidance based on deep reinforcement learning. Ocean Eng. 191, 106436.
Zhen, R., Riveiro, M., Jin, Y., 2017. A novel analytic framework of real-time multi-vessel collision risk assessment for maritime traffic surveillance. Ocean Eng. 145, 492–501.
Zhen, R., Shi, Z., Liu, J., Shao, Z., 2022a. A novel arena-based regional collision risk assessment method of multi-ship encounter situation in complex waters. Ocean Eng. 246, 110531 https://doi.org/10.1016/j.oceaneng.2022.110531.
Zhen, R., Shi, Z., Shao, Z., Liu, J., 2022b. A novel regional collision risk assessment method considering aggregation density under multi-ship encounter situations. J. Navig. 75, 76–94.